Table 1. Neuroblastoma cell lines used in this study

Cell line	*MYCN amplification*	*ALK status*
CHP-134	–	WT
GOTO	+	WT
LAN-1	+	F1174L
LAN-2	+	WT
LAN-5	+	R1275Q
NB-1	–	Amplification
NB-16	+	WT
NB-19	+	WT
NB-69	–	WT
NH-12	+	WT
SCMC-N2	+	F1174L
SCMC-N4	+	WT
SCMC-N5	+	K1062M
SJNB-1	–	WT
SJNB-2	+	R1275Q
SJNB-3	–	WT
SJNB-4	+	F1174L
SJNB-5	+	WT
SJNB-6	+	WT
SJNB-7	+	WT
SJNB-8	+	WT
SK-N-SH	–	F1174L
TGW	+	R1275Q
UTP-N-1	+	WT

Abbreviations: ALK, anaplastic lymphoma kinase; WT, wild type.

Structural abnormality of the *ALK* gene in NB-1 cells

As reported previously,[7] our single-nucleotide polymorphism array-based copy number analysis of NB-1 cells disclosed high-level gene amplification of the *ALK*-containing 2p24 segment. This should explain the high *ALK* expression observed in this cell line (Figures 1a and b). In particular, the genomic copy numbers within the 2p23 amplicon exhibited a transient decrease at three consecutive single-nucleotide polymorphisms (Chr2: 29 911 541–29 912 210), which corresponded to *ALK* intron 3, raising the possibility that a gene deletion involving exons 2 and 3 was responsible for the aberrant *ALK* transcript (Figure 2a). To confirm this, we performed Southern blot analysis of NB-1 genomic DNA using fragments exons 1–4 as probes (Figure 2b). As shown in Figures 2c–e, Southern blot analysis confirmed *ALK* gene amplification in NB-1 cells, as these blots showed high-intensity signals for each of the four *ALK*-specific probes in NB-1 cells compared with those in the controls. However, a significant difference was observed in the signal intensity between the fragments containing exons 1/4 and exons 2/3 in the NB-1 lanes, in which exons 1 and 4 showed 3.9- and 3.8-fold higher signals than exons 2 and 3, respectively. This result was confirmed by quantitative genomic PCR analysis using seven primer sets located within *ALK* exons 1–4 (Figure 2f). Taken together, these results indicate that the 2p23 amplicons were heterogeneous with regard to the species of *ALK* it contained, among which the predominant *ALK* allele had a deletion at exons 2 and 3, and these amplicons were responsible for the generation of $ALK^{del2\text{-}3}$.

Oncogenic potential of an aberrant short-form ALK protein

We next evaluated the oncogenic role of the truncated form of ALK found in NB-1 cells in terms of its kinase activity. As shown in Figure 3a, $ALK^{del2\text{-}3}$ was strongly phosphorylated in NB-1 cells, whereas the wild-type ALK expressed in NH-12 cells was unphosphorylated. Similar to the constitutive active F1174L ALK mutant when expressed in NIH3T3 cells, $ALK^{del2\text{-}3}$ had enhanced ALK phosphorylation compared with wild-type ALK (Figure 3b). Moreover, after anti-FLAG immunoprecipitation of FLAG-tagged ALK constructs, $ALK^{del2\text{-}3}$ and F1174L ALK mutants were strongly phosphorylated according to western blot analysis using a PY20 blot (Figure 3c). In addition, they exhibited enhanced kinase activity in an *in vitro* kinase assay using the YFF peptide as a substrate (Figure 3d). To confirm kinase activity of the $ALK^{del2\text{-}3}$ mutant, we further examined *in vitro* kinase activities of wild-type and mutant ALK-expressing NIH3T3 cells using a universal substrate. The immunoprecipitated FLAG-tagged $ALK^{del2\text{-}3}$ mutant showed significantly increased kinase activity (Supplementary Figure S1).

In an analysis of activated downstream signaling, significantly enhanced STAT3 phosphorylation was observed in $ALK^{del2\text{-}3}$ and F1174L mutants, whereas a significant increase in AKT phosphorylation was not detected in any samples (Figure 3e and Supplementary Figure S2). Extracellular regulated kinase (ERK) was probably phosphorylated in the F1174L mutant and wild-type ALK, but not in $ALK^{del2\text{-}3}$ (Figure 3e). The results of three independent experiments were quantified by densitometric scanning (Supplementary Figure S2).

We investigated the oncogenic potential of the $ALK^{del2\text{-}3}$ mutant in NIH3T3 cells, in terms of colony formation in soft agar and tumor generation in nude mice. As shown in Figures 4a and b, NIH3T3 cells that were stably transduced with $ALK^{del2\text{-}3}$ and ALK^{F1174L} produced a significantly higher numbers of colonies in soft agar than mock or wild-type *ALK*-transduced cells (Figures 4a and b). When inoculated into nude mice, the $ALK^{del2\text{-}3}$-transduced NIH3T3 cells invariably developed into subcutaneous tumors (5/5), whereas the mock and wild-type *ALK*-transfected cells did not develop into tumors (0/5) (Figure 4c).

$ALK^{del2\text{-}3}$ was retained in the endoplasmic reticulum

Among ALK signaling pathway molecules, STAT3 was only strongly phosphorylated by $ALK^{del2\text{-}3}$, suggesting that the $ALK^{del2\text{-}3}$ mutant was exclusively involved in the STAT3 pathway. It has been previously reported that intracellular fms-like tyrosine kinase-internal tandem duplication activation induces an aberrant downstream signaling outcome.[17] To determine whether $ALK^{del2\text{-}3}$ expresses at the cell surface and mediates signals from endoplasmic reticulum (ER), we analyzed localization and deglycosidation of $ALK^{del2\text{-}3}$ in NB-1 cells and wild-type ALK in NH-12 cells. Immunofluorescence staining revealed that ALK in NB-1 cells was almost colocalized with PDI, whereas ALK in NH-12 cells was largely located at the plasma membrane (Figure 5a). As shown in Supplementary Figure S4, colocalization of ALK and PDI was quantified using the Pearson's correlation coefficient. Moreover, to determine whether $ALK^{del2\text{-}3}$ was subjected to maturation of its oligosaccharides, we examined the endoglycosidase H sensitivity of ALK expressed in NB-1 and NH-12 cells. As shown in Figure 5b, $ALK^{del2\text{-}3}$ in NB-1 cells revealed the high sensitivity of endoglycosidase H compared with the wild-type ALK in NH-12 cells, suggesting that intercellular localization of $ALK^{del2\text{-}3}$ was associated with a defect in N-linked glycosylation.[18] These results indicate that $ALK^{del2\text{-}3}$ is mainly located at ER and aberrantly activates the STAT3 pathway from there.

Effect of ALK inhibition on cell growth in NB-1 cells

Finally, we examined the effect of ALK inhibition on NB-1 cell proliferation using the small-molecule ALK inhibitor TAE684 and siRNA-mediated ALK knockdown. NB-1 cell growth was effectively inhibited by TAE684 with a half maximal inhibitory concentration (IC_{50}) of 13 nM, which was similar to the IC_{50} for SK-N-SH (49 nM; an *ALK*-mutated TAE684-sensitive neuroblastoma cell line), but substantially lower than the IC_{50} for TGW cells with the ALK^{R1275Q} mutant (310 nM), the glioblastoma-derived cell line H4 with wild-type ALK (190 nM) and NIH3T3 cells with no ALK expression (380 nM) (Figure 6a). Similarly, siRNA-mediated knockdown of $ALK^{del2\text{-}3}$ in NB-1 cells resulted in significant suppression of cell proliferation compared with controls transfected with nonspecific

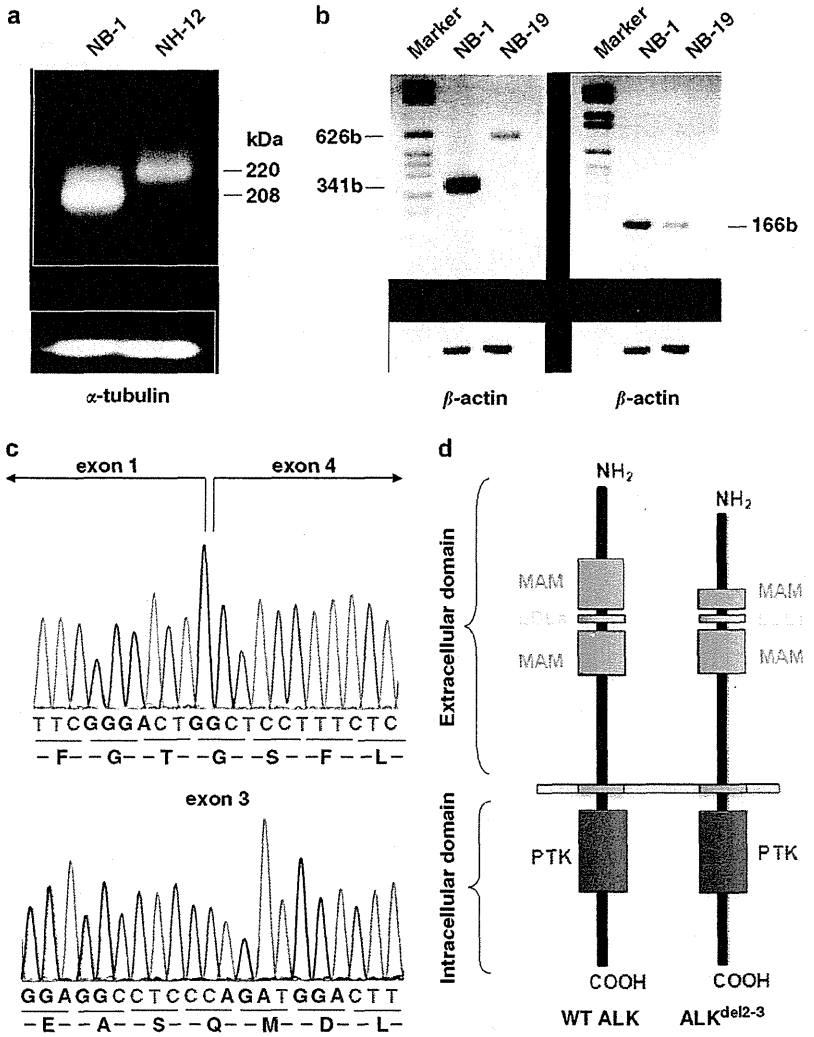

Figure 1. Detection of an aberrant truncated form of ALK in NB-1 cells. (**a**) Western blot analysis of ALK in neuroblastoma-derived cell lines. NB-1 cells strongly expressed the truncated form with a molecular mass of 208 kDa. In contrast, wild-type ALK-expressing neuroblastoma-derived cell lines (NH-12) revealed an ALK protein with a molecular mass of 220 kDa. α-Tubulin staining as loading control. (**b**) RT-PCR analysis of *ALK* exons 1–5 and exons 2 and 3 in the neuroblastoma cell lines. A short PCR product with 314 bp was detected in NB-1 cells, whereas much longer PCR products with 627 bp were detected in NB-19 cells with wild-type *ALK*. Wild-type *ALK* was detected in both NB-1 and NB-19 cells using *ALK* exon 2 and 3 primers. (**c**) Subsequent sequence analysis of *ALK* cDNA from NB-1. In-frame deletion in exons 2 and 3 was confirmed by direct sequencing. Sequencing of the PCR product detected by RT-PCR for *ALK* exons 2 and 3 confirmed the presence of wild-type *ALK* in NB-1 cells. Lower panel represents DNA sequencing for *ALK* exon 3 in NB-1 cells. (**d**) Schematic representation of the truncated form of aberrant ALK. The extracellular domain of ALK comprises two MAM domains (aa 264–427 and 480–626), one low-density lipoprotein class A (LDLa) motif (aa 453–471) and a glycine-rich region (aa 816–940) (Palmer *et al.*[30]). Because exons 2 and 3 of *ALK* implicate 224–318 aa, the in-frame deleted mutant led to a translational truncated form of the first MAM domain. PTK, protein tyrosine kinase.

siRNA, but the suppression apparently decreased in wild-type ALK-expressing NH-12 cells (Figures 6b and c). As shown in Supplementary Figure S3, significant inhibition was observed in NB-1 cells with ALK knockdown compared with that in the negative control ($P<0.05$, Mann-Whitney *U*-test).

DISCUSSION

Deregulated activation of ALK has been implicated in various human cancers through either generation of fusion proteins, overexpression or single amino-acid changes. In this study, we described a novel mechanism of oncogenic activation of *ALK* that operated in a neuroblastoma-derived cell line, NB-1. In NB-1 cells, an aberrant form of *ALK* that lacks exons 2 and 3 was amplified, leading to high-level expression of an N-terminal-truncated kinase, ALK^{del2-3}, and our functional studies confirmed the oncogenic role of ALK^{del2-3}. First, ALK^{del2-3} underwent autophosphorylation in NB-1 and NIH3T3 cells and demonstrated enhanced kinase activity, promoting downstream signaling pathways such as the STAT3 pathway. Second, ALK^{del2-3} promoted colony formation in soft agar and tumorigenicity when transduced into NIH3T3 cells in nude mice. Finally, inhibition of cell growth was observed when we treated NB-1 cells with TAE684, an ALK-specific kinase inhibitor, and siRNA-mediated gene knockdown. Unfortunately, screening of 71 primary neuroblastoma specimens and 23 neuroblastoma-derived cell lines did not identify a similar mechanism of ALK oncogenic activation in neuroblastoma; therefore, it is not a common mechanism for ALK activation in

Table 2. Neuroblastoma fresh tumor samples used in this study

Clinicopathological findings	*Samples*
Age (years)	
>1	41
<1	30
Stage	
1	16
2	11
3	12
4	29
4S	2
ND	1
MYCN status	
Amplification (+)	11
(−)	58
ND	2
ALK status	
Amplification	1
Mutation	6
Wild type	64
Total	71

Abbreviations: ALK, anaplastic lymphoma kinase; ND, not determined.

neuroblastoma. Nevertheless, the discovery of this unique ALK form will add to our knowledge with regard to the pathogenesis of neuroblastoma and will help to elucidate the mechanism of ALK activation.

Abnormal activation of RTK through a deletion in its extracellular domain has been documented in several cancers.[19-21] A common example of abnormal RTK activation is the epidermal growth factor receptor class III variant, which is present in a substantial proportion of malignant gliomas and other human cancers, but completely absent in normal tissues.[22,23] This variant results from a transcript having an 801-bp in-frame deletion of EGFR that corresponds to exons 2–7, which leads to the generation of a protein with a truncated extracellular domain.[21,24] Several molecular mechanisms have been implicated in the oncogenic pathway with epidermal growth factor receptor class III variant downstream signaling.[21,24] For example, in addition to ligand-independent self-dimerization, epidermal growth factor receptor class III variant has been shown to constitutively interact with adaptor proteins SHC and GRB2, which are involved in the recruitment of the RAS pathway.[25] The recepteur d'origine nantais (RON) RTK variant with a deletion in the first immunoglobulin-plexin transcription domain (RONΔ160) has also been considered as a constitutively activated kinase in several human cancers.[20,26] RON belongs to the MET proto-oncogene family, which plays a critical role in epithelial cell homeostasis and tumorigenic development.[27] RONΔ160 is derived from a *RON* mRNA transcript by alternative splicing that eliminates 109 aa residues from the extracellular domain of RON β-chain and is expressed in >50% of primary colon cancers and 90% of brain tumors, but not in any normal tissues.[26,28] The deleted 109 aa residues are encoded by exons 5/6, which constitute the first immunoglobulin-plexin transcription domain in the RON β-chain.[26,28] The mechanism for the oncogenic activation of RONΔ160 is believed to be one in which the deletion in the extracellular domain causes conformational changes in the kinase and leads to spontaneous dimerization, which in turn causes constitutive receptor phosphorylation and increased intracellular signaling activation.[26,28,29]

The $ALK^{del2\text{-}3}$ variant consists of a 282-bp in-frame deletion of *ALK* that corresponds to 224–318 aa in the first MAM domain (Figure 1d). ALK is the sole RTK that contains MAM domains in its extracellular region.[30] Although MAM domains are thought to participate in cell–cell interactions, their significance in ALK function remains unclear.[15,16] Thus, the functional significance of MAM deletion in the truncated ALK is still elusive. As the deleted region of *ALK* detected in NB-1 cells is in close proximity to a ligand-binding domain (391–401 aa), this deletion may structurally alter the ligand-binding domain. Similar to epidermal growth factor receptor class III variant and RONΔ160, the $ALK^{del2\text{-}3}$ variant may be constitutively activated in a ligand-independent manner and/or through spontaneous dimerization, although the exact mechanism of constitutive activation of $ALK^{del2\text{-}3}$ is yet to be elucidated.

Oncogenic ALK transformation is mediated by interactions with downstream molecules that trigger a substantial intercellular signaling cascade.[31] The most relevant and best-characterized ALK downstream pathways are the RAS-ERK, JAK3-STAT3 and PI3K-AKT pathways.[31] Among ALK signaling molecules, STAT3 is only strongly phosphorylated by $ALK^{del2\text{-}3}$, suggesting that besides F1174L or K1062M ALK mutants,[7] $ALK^{del2\text{-}3}$ would be exclusively involved in the STAT3 pathway. Recently, it has been reported that the oncogenic mutant of fms-like tyrosine kinase-internal tandem duplication aberrantly activates STAT5 when localized at ER, but fails to activate MAPK and AKT signaling.[17] Thus, this raises the possibility that involvement of the STAT3 pathway in $ALK^{del2\text{-}3}$-expressing cells resembles the fms-like tyrosine kinase-internal tandem duplication mutant.[17] Immunofluorescence staining and the endoglycosidase H sensitivity assay revealed that $ALK^{del2\text{-}3}$ is mainly located at ER and aberrantly activates the STAT3 pathway from ER. Taken together, our results suggest that intracellular activation of $ALK^{del2\text{-}3}$ switches downstream signaling to the ALK pathway.[18]

Furthermore, ERK phosphorylation was similarly elevated in cells expressing wild-type or F1174L ALK. This may have been because of enhanced expression of exogenous wild-type *ALK* by retrovirus-mediated gene transfer. Schulte *et al.*[32] reported that the high level of wild-type ALK and mutant ALK expression has similar effects on the neuroblastoma biological phenotype, which may be related to tumor growth. Taken together, the results from our study and from the study by Schulte *et al.*[32] suggest that in addition to the ALK mutants, elevated wild-type ALK expression also mediates similar molecular functions that contribute to the malignant phenotype in neuroblastoma.

In summary, we found that an N-terminal-truncated ALK protein observed in a neuroblastoma-derived cell line (NB-1) is a novel oncogenic isoform of ALK. This study provides a better understanding of the molecular mechanism of pathogenesis of neuroblastoma as well as oncogenic roles of ALK pathway.

MATERIALS AND METHODS

Specimens

In all, 24 neuroblastoma cell lines were used in this study (Table 1). The SCMC-N series was established in our laboratory.[33] The SJNB series and UTP-N-1 cells were provided by Dr AT Look and Dr A Inoue, respectively. Other cell lines were obtained from the Japanese Cancer Resource Cell Bank (http://cellbank.nibio.go.jp/wwwjcrbj.htm). All cells were maintained in RPMI 1640 medium (Gibco, Grand Island, NY, USA) supplemented with 10% fetal bovine serum in a humidified atmosphere containing 5% CO_2 at 37 °C. Primary neuroblastoma specimens were obtained through surgery or biopsy from patients who were diagnosed with neuroblastoma and who were admitted to Tokyo University Hospital, Saitama Children's Medical Center or various other hospitals between November 1993 and October 2006. The patients were staged according to the International Neuroblastoma Staging System,[34] and the clinicopathological findings are listed in Table 2.

ALK expression analyses

Total cellular proteins were resolved on a 5–10% gradient sodium dodecyl sulfate–polyacrylamide gel and electrophoretically transferred onto

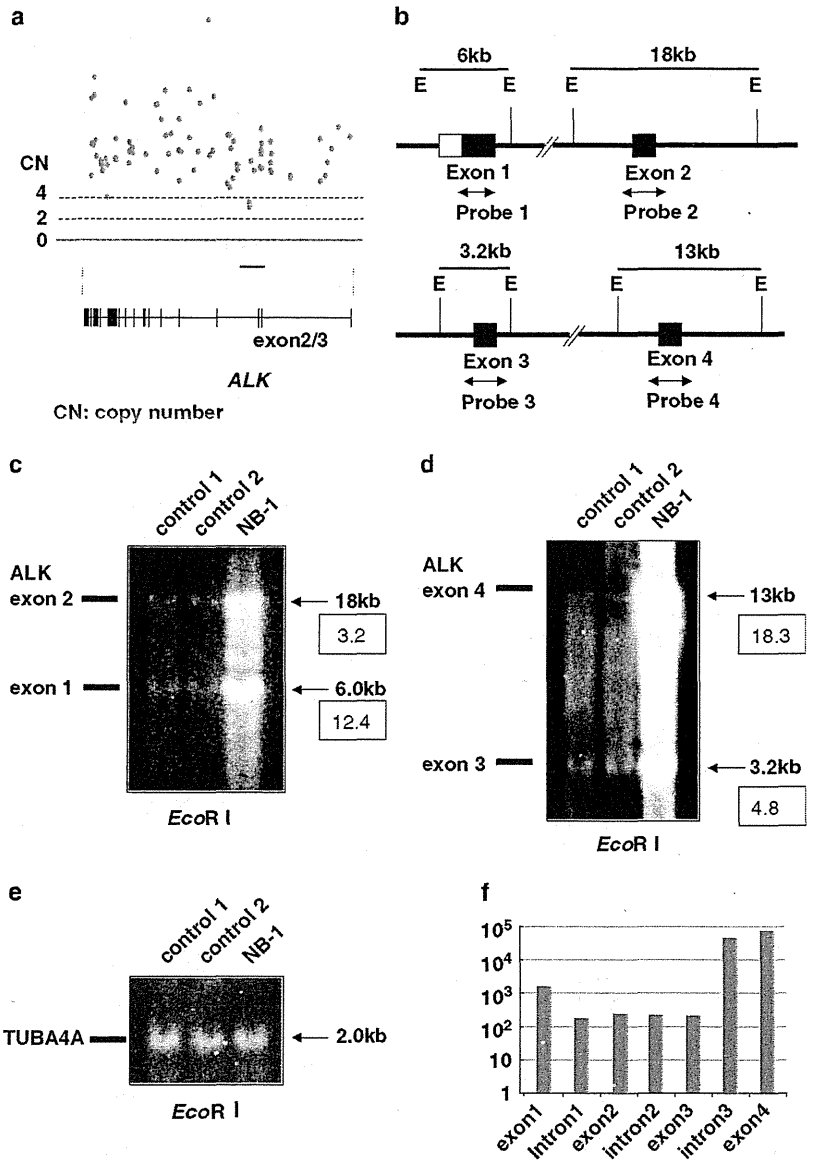

Figure 2. Genetic characteristics of the N-terminal-truncated form of ALK. (**a**) High-grade amplification of the *ALK* locus detected in NB-1 cells by single-nucleotide polymorphism array analysis (Affymetrix GeneChip 250k *Nspl*). Among the single-nucleotide polymorphism probes located within the *ALK* amplicon, three consecutive single-nucleotide polymorphism probes (Chr2: 29 911 541 and 29 912 210) located within *ALK* intron 3 showed relatively low signal intensities. The red line indicates the focal deletion within *ALK* intron 3. (**b**) Physical maps of *ALK* exons 1–4. The restriction sites and probe maps for *ALK* exons 1–4 are indicated. E: *EcoR*1. Arrows indicate probe positions. (**c**, **d**) Southern blot analysis using *ALK* exon 1–4 probes (**c**: exons 1 and 2; **d**: exons 3 and 4). Normal peripheral blood DNA was used as a germline control. Densitometric analysis was performed using the ImageQuant 400 and ImageQuant TL software version 7. (**e**) The TUBA4A probe was used as a loading control. (**f**) Quantitative genomic PCR analysis of *ALK* using seven primer sets located within *ALK* exons 1–4. The signal intensities of *ALK* introns 1 and 2 and exons 2 and 3 were lower compared with those of *ALK* exons 1 and 4 in NB-1 cells.

polyvinylidene difluoride membranes. After blocking with 5% milk in Tris-buffered saline containing 0.1% Tween (10 mM Tris-HCl (pH 7.4), 150 mM NaCl and 0.1% Tween-20), membranes were incubated for 1 h with primary antibody in TBS-T, washed and incubated for 12 h with primary antibody in 3% bovine serum albumin. The membranes were then washed again and incubated with anti-rabbit immunoglobulin G at room temperature for 1 h. Subsequently, they were extensively washed, and the proteins were visualized by enhanced chemiluminescence (Millipore, Bedford, MA, USA). Total RNA was extracted from the 24 cell lines and 71 frozen stocked tumors using Isogen reagent (Nippon Gene, Osaka, Japan) according to the manufacturer's instructions; the total RNA was analyzed by RT-PCR to synthesize cDNA using the SuperScript Preamplification System for first-strand cDNA synthesis (Life Technologies Inc., Rockville, MD, USA). RT-PCR analysis for *ALK* expression was performed as described previously,[7] using the primer sets listed in Table 3. cDNA concentration was equalized using *β-actin* expression as a control.

Southern blot analysis

High-molecular-weight DNA was prepared from cells according to standard procedures using the QIAamp DNA Mini kit (Qiagen, Valencia, CA, USA) and a modification of the protocol provided by the manufacturer.

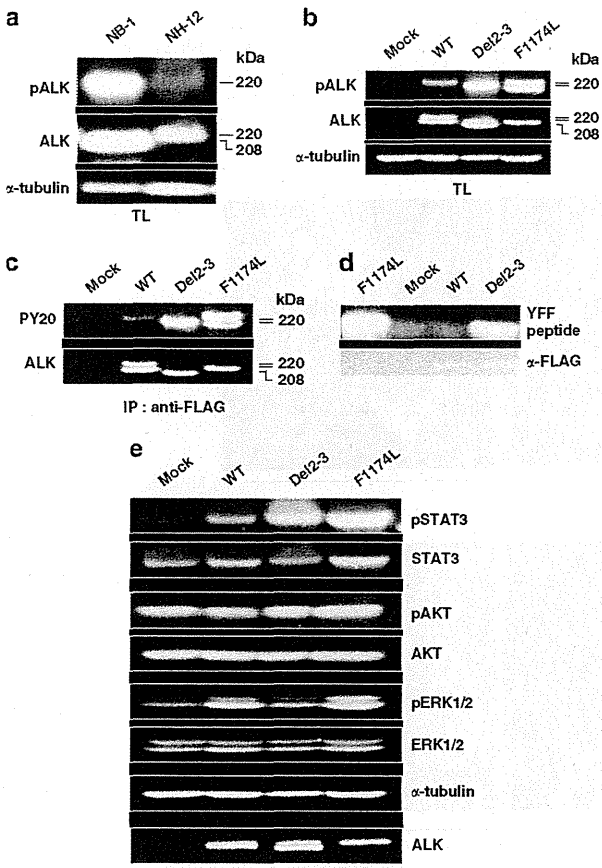

Figure 3. Kinase activities of ALK mutants and their downstream status. (**a**) Western blot analysis of ALK and phosphorylated ALK in NB-1 and NH-12 cells. NB-1 cells strongly expressed the truncated form of ALK and phosphorylated ALK compared with that in NH-12 cells. TL: Total cell lysates. (**b**) Western blot analysis of NIH3T3 cells stably expressing ALK mutants (ALK^{del2-3} and ALK^{F1174L}) and wild-type ALK. (**c**) Stably expressed ALK mutants and wild-type ALK were immunoprecipitated with an anti-FLAG antibody and subjected to western blot analysis with anti-PY20. (**d**) *In vitro* kinase assay for wild-type ALK and its mutants using the synthetic YFF peptide as a substrate. (**e**) Western blot analysis of NIH3T3 cells stably expressing ALK mutants and wild-type ALK for their downstream effectors, STAT3 (pSTAT3), AKT (pAKT) and ERK (pERK). The total amount of each molecule is also shown together with an α-tubulin blot.

DNA was extracted from NB-1 cells and peripheral normal blood cells. For Southern blot analysis, 10 μg genomic DNA was restricted with *Eco*RI and loaded onto an agarose gel.[35] After electrophoresis, the DNA was transferred to polyvinylidene difluoride membranes and hybridized with radiolabeled probes for *ALK* exons 1–4 listed in Table 3. The signal intensity of each band was quantified and calculated using the ImageQuant 400 and ImageQuant TL software version 7 (GE Healthcare, Piscataway, NJ, USA).

Quantitative genomic PCR analysis

Quantitative genomic real-time PCR was performed using SYBR Green-based quantification (Bio-Rad Laboratories, Hercules, CA, USA). The standard curve method was used to calculate the target genome numbers in the NB-1 cell line. The relative target copy number was normalized to normal human genomic DNA as a calibrator. The primer sequences used for quantitative genomic PCR are shown in Table 3.

Transforming potential of ALK mutants

ALK^{WT}-FLAG and ALK^{F1174L}-FLAG were FLAG-tagged cDNAs for wild-type *ALK* and its F1174L mutant, respectively. FLAG-tagged cDNA for the

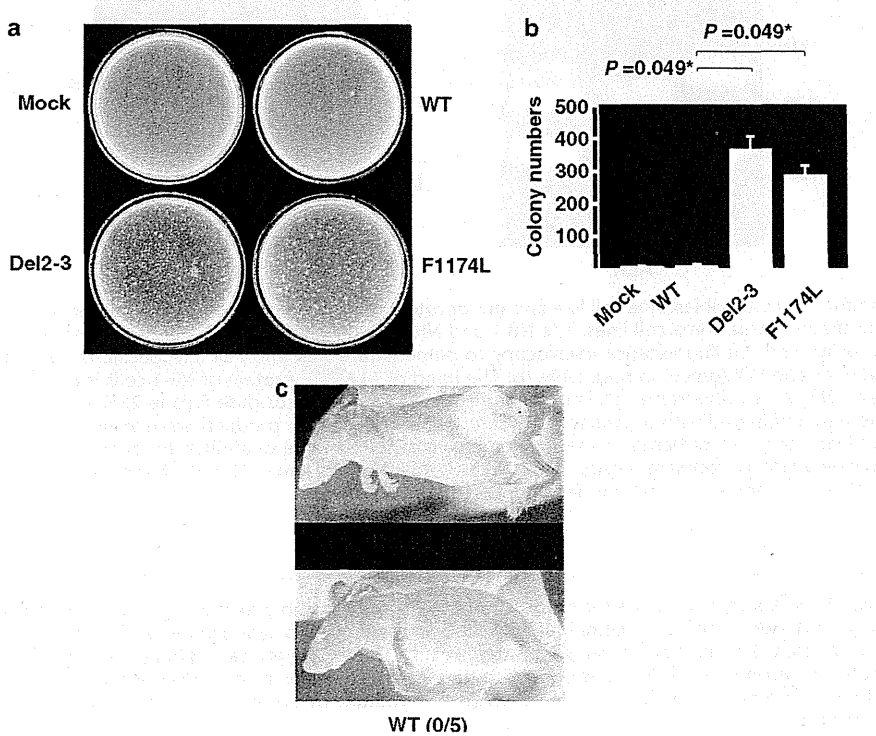

deletion mutant (*ALK*$^{del2\text{-}3}$-FLAG) was isolated from total RNA of NB-1 cells by high-fidelity PCR. After re-sequencing, each cDNA was constructed into the pcDNA3 expression plasmid and transfected into NIH3T3 cells using Effectene Transfection Reagents (Qiagen, Tokyo, Japan). Kinase assays were performed with stable clones in these constructs. For western blot analysis of mutant ALK and colony formation assays, NIH3T3 cells were stably transduced with wild-type and mutant ALK by retrovirus-mediated gene transfer. FLAG-tagged cDNA for wild-type and mutated ALK were then

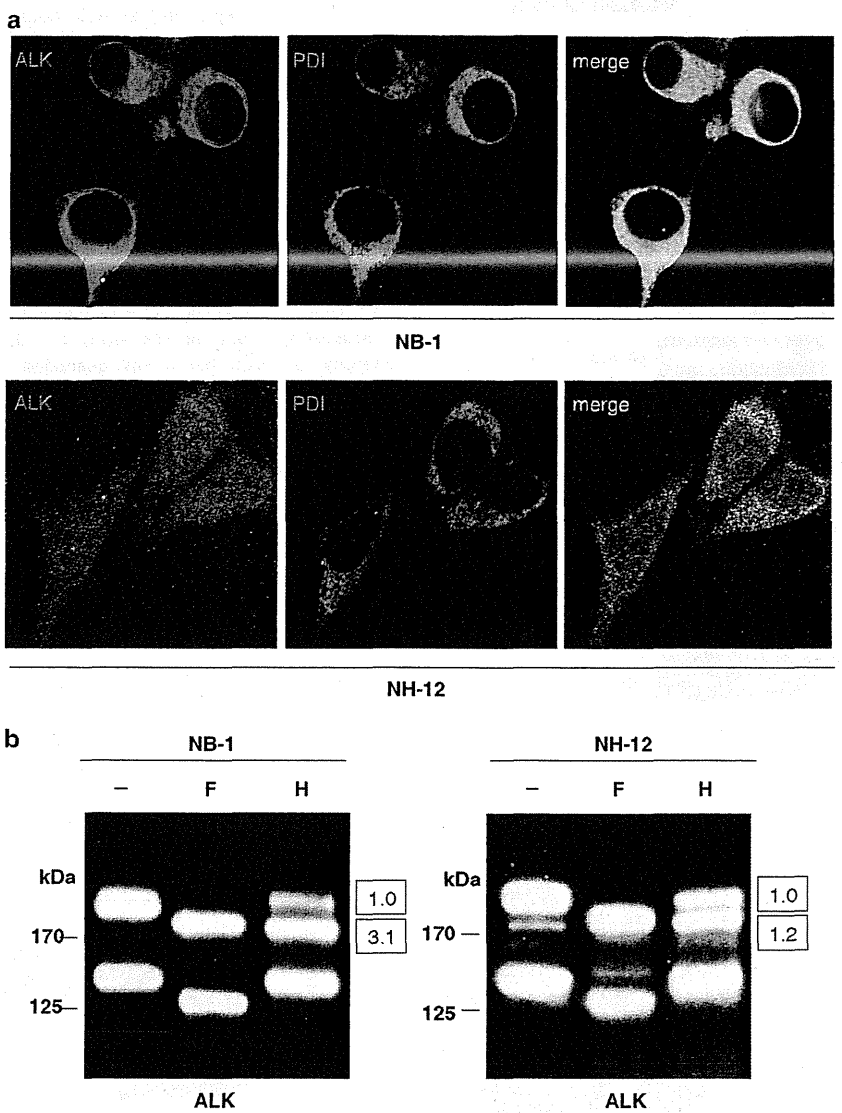

Figure 5. ER retention in the NB-1 neuroblastoma cell line and glycoprotein maturation. (**a**) Immunofluorescence confocal microscopy analysis of ALK ER localization in the neuroblastoma cell lines. The NB-1 and NH12 neuroblastoma cell lines were immunostained with the indicated antibodies and imaged using immunofluorescence microscopy to demonstrate ALK and PDI (ER-specific marker) colocalization. Cells were immunostained for ALK (red) and PDI (green), respectively. (**b**) The band of ALK$^{del2\text{-}3}$ protein of NB-1 cells is endoglycosidase H sensitive. Cell lysates from the NB-1 and NH12 neuroblastoma cell lines were incubated with N-glycosidase F (lane 2, F) and endoglycosidase H (lane 3, H). Deglycosidation profiles were compared with untreated cell lysates (lane 1). Digestion products were analyzed by western blot analysis using monoclonal anti-ALK. Signal intensities of bands in the lane endoglycosidase H were quantified by densitometric scanning using the ImageQuant 400 and ImageQuant TL software version 7. Signal intensity of approximate190 kDa band that revealed sensitivity to endoglycosidase H in NB-1 cells showed 3.1-fold higher than that of upper band.

Figure 4. Oncogenic role of the aberrant truncated form of ALK. (**a**) NIH3T3 cells stably expressing mutant kinases (ALK$^{del2\text{-}3}$ and ALK^{F1174L}) showed increased colony formation in soft agar compared with cells expressing wild-type kinase. (**b**) The average numbers of colonies in triplicate experiments are plotted. Standard deviation is indicated. Results showing significant differences compared with experiments using wild-type ALK are indicated by asterisks with *P*-values. (**c**) *In vivo* tumorigenicity assay in nude mice. Tumor formation assay in nude mice in which 1.0×10^7 NIH3T3 cells expressed wild-type ALK and the ALK$^{del2\text{-}3}$ mutant by the calcium phosphate method. Tumor formation was evaluated 21 days after inoculation.

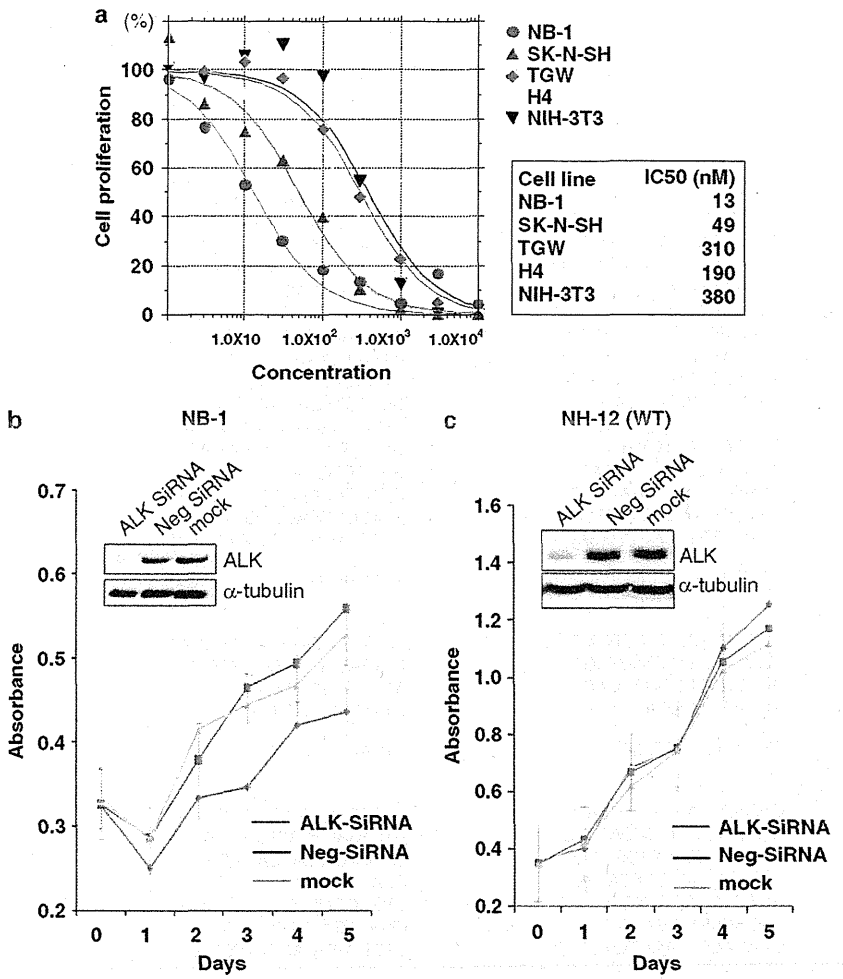

Figure 6. Effect of ALK inhibition on NB-1 cell proliferation using the ALK inhibitor TAE684 and siRNA-mediated ALK knockdown. (**a**) NB-1 cell growth was effectively inhibited by TAE684, with an IC_{50} similar to that for SK-N-SH (an *ALK*-mutated TAE684-sensitive neuroblastoma cell line), but substantially lower than that for NIH3T3 cells with no ALK expression. (**b**, **c**) Effect of RNAi-mediated ALK knockdown on cell proliferation in neuroblastoma cell lines expressing either the $ALK^{del2\text{-}3}$ mutant (NB-1) or wild-type ALK (NH-12). Cell growth was measured using the Cell Counting kit-8 after knockdown experiments using ALK-specific siRNAs, negative control siRNAs or mock experiments, in which absorbance was measured in triplicate and averaged for each assay. The mean ± s.d. of the average absorbance in three independent knockdown experiments was plotted to draw the growth curves. Successful knock down of the ALK protein was confirmed by anti-ALK blots using α-tubulin blots as controls.

constructed in the pGCDNsamIRESKO retrovirus vector. Vector plasmids were co-transfected with vesicular stomatitis virus-G cDNA into 293GP cells to obtain a retrovirus-containing supernatant, which was then transduced into 293GPG cells to stable cell lines capable of producing vesicular stomatitis virus-G-pseudotyped retroviral particles on induction.

Functional analyses of a short-form ALK

To evaluate the phosphorylation status of the ALK mutants, stable clone cell lysates were subjected to western blot analysis with anti-ALK and the antibody-specific pTyr1604 (Cell Signaling Technology, Danvers, MA, USA) of ALK. Immunoprecipitation with antibodies to FLAG (Sigma, St Louis, MO, USA) were subjected to western blot analysis with a generic antiphosphotyrosine antibody (PY20). Western blot analyses were also performed using anti-ERK1/2, anti-phospho-ERK1/2, anti-AKT, anti-phospho-AKT, anti-STAT3 and anti-phospho-STAT3 antibodies (Cell Signaling Technology). AKT and STAT3 phosphorylation signals were quantitated by densitometric scanning using the ImageQuant 400 and ImageQuant TL software version 7 (GE Healthcare). The *in vitro* kinase assay was performed with the synthetic YFF peptide (Operon Biotechnologies, Reutlingen, Germany), as described previously,[36] using stable clones in pcDNA vector constructs. We also used the *in vitro* kinase assay for wild-type and mutant *ALK* expression in NIH3T3 cells by retrovirus-mediated gene transfer using the poly-GluTyr peptide. Cell extracts were immunoprecipitated with anti-Flag antibody, and the expression was subjected to immunoblotting using anti-ALK antibody. ALK mutant kinase activity was measured using a non-radioactive isotope solid-phase enzyme-linked immunosorbent assay in the Universal Tyrosine Kinase Assay kit (Takara Bio, Osaka, Japan). Assays were performed in 40 mM Tris (pH 7.4), 20 mM $MgCl_2$, 2 mM dithiothreitol and 0.1 mg/ml bovine serum albumin buffer.

Transforming potential of short-form ALK

For colony assays, 1×10^3 stably transfected NIH3T3 cells were mixed in 0.4% agarose with 10% fetal bovine serum-Dulbecco's modified Eagle's medium and plated on 0.6% agarose-coated 35-mm dishes. After culturing for 14 days, colonies measuring 0.1 mm in diameter were counted. Colonies were quantified during triplicate experiments. Tumor formation

Table 3. Primer sets used in this study

	Primer sequence (5′→3′)		*Annealing temperature (°C)*
	Forward	*Reverse*	
RT-PCR analyses			
ALK exon 1/5	CTTCTCTTCCAGATCTTCGG	ATTCAGGGCAAAGAAGTCCAC	55
Exon 1/2	AAGCAGTTGGTGCTGGAGCT	TTTGACTTCCCCTGTGAGCT	55
Exon 2/4	CATAGCTCCTTGGAATCACC	ATGAGGAGCAGCAGTGAGCA	55
Exon 4/5-6	TTCTCAACACCTCAGCTGAC	ACTGCAGTGAAGGAACATCC	55
Exon 5/8-9	GAAACCGCAGCTTGTCTGCA	CGATCAAGAGCTCTCCATGT	55
Exon 8/12	AAGTGCTACAGTGACCAGTG	TAGCGGAGAGGACAAGATC	55
Exon 11/14	ATATCTCCATCAGCCTGGAC	AAGAACACCATGATGCGGTC	55
Exon 13/15-16	CCTGAAAGGCATCCAGATCT	AAGATGAAGGATGGAGTGCC	55
Exon 15/17	AATCCGTGTGAACAGAAGCG	TGGAGGAGGCGGAGGATATA	55
Exon 17/19-20	AAATCTTTGCAGGAGGGTGC	GCGTCTCCTGCATTGTGTCA	55
Exon 20/23	TTTCTCCGGCATCATGATTG	CTCATGGAAGCCCTGATCAT	55
Exon 23/26	TGCCTGAAGTGTGCTCTGAA	GATTGGAGACTTCGGGATGG	55
Exon 26/30	AGAAACTGCCTCTTGACCTG	GGACCCGGATGTAATCAACA	55
Exon 29/30	GGAGAGGATTGAATACTGCA	GTTGCACAAGGTCCACGGAT	55
Exon 30/30	TGCAGAGATCTCTGTTCGAG	GTTGCACAAGGTCCACGGAT	55
Exon 30/30	TAACGTTGCAACTGGGAGAC	GTTGCACAAGGTCCACGGAT	55
β-Actin	CTTCTACAATGAGCTGCGTG	TCATGAGGTAGTCAGTCAGC	55
Southern blot analyses			
ALK exon 1	AGAGTCTGGCAGTTGACTTC	TGCTCACAAACAGTCCCGAAG	60
Exon 2	TCAACTCAGTCTACTGGTGG	GGATATGGCAGACACAAAGC	60
Exon 3	AGCCCTGTGGTATTGACAAC	AGATGGGACTTGTCTTCCTC	60
Exon 4	AGAATGGAGGAAGAAGGCTG	GTAATTGCTCAACCTGGACC	60
TUBA4A	CTCTCACACTCTGGTATCTC	CTGACCATTAGCACAGTCTC	60
Quantitative genomic PCR analyses			
ALK exon 1	CTCAGCGAGCTGTTCAGTTG	CAGTCCCGAAGATCTGGAAG	55
Intron 1	CTGCTTGGTTCCTCACATCC	GTCTGAGTCATTGGCTAATCTCA	55
Exon 2	ACCCAAGCACATGGATCAG	GATGAGACAGGAAAGGGAAGG	55
Intron 2	GGTATACACGTGCCATGGTG	CCAAATACGGCATGTTCTCA	55
Exon 3	GGAGTGCAGCTTTGACTTCC	CTGGGCATCTCCTTAGAACG	55
Intron 3	TGGCATGATTGATTACCCAAG	CTGGAGATCACCCTTTGAGG	55
Exon 4	CAACACCTCAGCTGACTCCA	CTCTCTTGCAGCCTCGTTG	55

Abbreviations: ALK, anaplastic lymphoma kinase; RT-PCR, reverse transcription-polymerase chain reaction.

assay was performed in nude mice, in which 1.0×10^7 NIH3T3 cells expressing wild-type *ALK* and $ALK^{del2\text{-}3}$ mutant were injected by the calcium phosphate method. Tumor formation was evaluated 21 days after inoculation as described previously.[6]

Immunofluorescence

Cells were fixed for 10 min with 4% paraformaldehyde and washed three times with phosphate-buffered saline. After 1 h of blocking in phosphate-buffered saline containing 4% donkey serum and 0.1% Triton X-100/phosphate-buffered saline, the cells were incubated for 2 h in the same buffer with polyclonal anti-ALK (Santa Cruz Biotechnology, Santa Cruz, CA, USA) and monoclonal anti-PDI (Abcam, Cambridge, MA, USA), respectively. The cells were then washed three times with phosphate-buffered saline before and after incubation with anti-mouse IgG Alexa Fluor 488 and anti-rabbit IgG Alexa Fluor 594-conjugated secondary antibodies, respectively, (Invitrogen, Carlsbad, CA, USA). The cells were then mounted in Prolong Gold (Invitrogen). Confocal laser microscopy was performed using a Fluoview 10 000 confocal microscope (Olympus, Tokyo, Japan). Colocalization of ALK and PDI was quantified using the Pearson's correlation coefficient and determined through correlation analysis with a Fluoview 1000 software.[37]

Deglycosylation of ALK with N-glycosidase F, N-glycosidase H and O-glycosidase

Proteins from cell lysates obtained from neuroblastoma cell lines NB-1 and NH-12 were incubated with N-glycosidase F and endoglycosidase H for deglycosylation (New England Biolabs, Ipswich, MA, USA), following the manufacturer's instructions.[18] The samples were then used for immunoblotting with anti-ALK antibody. Signal intensities of bands in the lane endoglycosidase H were quantified by densitometric scanning using the ImageQuant 400 and ImageQuant TL software version 7.

ALK inhibition by an ALK inhibitor and siRNA-mediated knockdown in neuroblastoma cells

A partial *ALK*-deleted neuroblastoma-derived cell line (NB-1), *ALK*-mutated neuroblastoma-derived cell lines (SK-N-SH and TGW) and a glioblastoma-derived cell line (H4) were cultured with varying concentrations of the ALK inhibitor TAE684,[8] and cell growth was measured using the CellTiter-Glo Luminescent Cell Viability Assay (Promega, Tokyo, Japan). NIH3T3 cells were used as a control. The IC_{50} value of TAE684 against NB-1 cells was calculated by nonlinear regression (variable slope) using the GraphPad Prism 5 software (GraphPad, La Jolla, CA, USA). NB-1 and NH-12 cells with wild-type ALK were transfected with either an *ALK*-specific siRNA or a nonspecific siRNA, as described previously.[7] To assess the effect of ALK knockdown on cell growth, cells were seeded in 96-well plates at a concentration of 1.0×10^4 cells per well 24 h before transfection and assayed using the Cell Counting kit-8 (Dojindo, Kumamoto, Japan). We also performed an siRNA-mediated ALK knockdown cell proliferation assay using a cell counter and 6-well plates. These cells were seeded in 6-well plates at a concentration of 2.0×10^5 cells per well 24 h before transfection. The number of cells was counted after 72 h using cytorecon (ECI, Tokyo, Japan).

Statistical analyses

The Mann-Whitney *U*-test was used to compare the differences in colony formation as well as the effects of ALK knockdown on cell growth between wild-type and ALK mutants. Phosphorylation signals of downstream molecules were evaluated by Student's *t*-test.

CONFLICT OF INTEREST

The authors declare no conflict of interest.

ACKNOWLEDGEMENTS

We thank Mrs Matsumura, Mrs Hoshino, Mrs Yin, Miss Ogino and Mrs Saito for their excellent technical assistance. We would also thank Dr Tanaka, Dr Saito, Mr Shiosaka and Mrs Mori for useful advice concerning biological analysis; Dr AT Look, Harvard Medical University, and Dr A Inoue, St Jude Children's Research Hospital, for their generous gifts of neuroblastoma cell lines. This work was supported by Research on Measures for Intractable Diseases, Health and Labor Sciences Research Grants, Ministry of Health, Labor and Welfare, Research on Health Sciences focusing on Drug Innovation, the Japan Health Sciences Foundation and Core Research for Evolutional Science and Technology, Japan Science and Technology Agency.

REFERENCES

1 Morris SW, Kirstein MN, Valentine MB, Dittmer K, Shapiro DN, Look AT *et al.* Fusion of a kinase gene, ALK, to a nucleolar protein gene, NPM, in non-Hodgkins-lymphoma (Vol 263, PG 1281, 1994). *Science* 1995; **267**: 316-317.
2 Shiota M, Nakamura S, Ichinohasama R, Abe M, Akagi T, Takeshita M *et al.* Anaplastic large-cell lymphomas expressing the novel chimeric protein P80(NPM/ALK)-a distinct clinicopathological entity. *Blood* 1995; **86**: 1954-1960.
3 Griffin CA, Hawkins AL, Dvorak C, Henkle C, Ellingham T, Perlman EJ. Recurrent involvement of 2p23 in inflammatory myofibroblastic tumors. *Cancer Res* 1999; **59**: 2776-2780.
4 Jazii FR, Najafi Z, Malekzadeh R, Conrads TP, Ziaee AA, Abnet C *et al.* Identification of squamous cell carcinoma associated proteins by proteomics and loss of beta tropomyosin expression in esophageal cancer. *World J Gastroenterol* 2006; **12**: 7104-7112.
5 Rikova K, Guo A, Zeng Q, Possemato A, Yu J, Haack H *et al.* Global survey of phosphotyrosine signaling identifies oncogenic kinases in lung cancer. *Cell* 2007; **131**: 1190-1203.
6 Soda M, Choi YL, Enomoto M, Takada S, Yamashita Y, Ishikawa S *et al.* Identification of the transforming EML4-ALK fusion gene in non-small-cell lung cancer. *Nature* 2007; **448**: 561-5U3.
7 Chen YY, Takita J, Choi YL, Kato M, Ohira M, Sanada M *et al.* Oncogenic mutations of ALK kinase in neuroblastoma. *Nature* 2008; **455**: 971-U56.
8 George RE, Sanda T, Hanna M, Frohling S, Luther W, Zhang JM *et al.* Activating mutations in ALK provide a therapeutic target in neuroblastoma. *Nature* 2008; **455**: 975-978.
9 Janoueix-Lerosey I, Lequin D, Brugieres L, Ribeiro A, de Pontual L, Combaret V *et al.* Somatic and germline activating mutations of the ALK kinase receptor in neuroblastoma. *Nature* 2008; **455**: 967-U51.
10 Mosse YP, Laudenslager M, Longo L, Cole KA, Wood A, Attiyeh EF *et al.* Identification of ALK as a major familial neuroblastoma predisposition gene. *Nature* 2008; **455**: 930-U22.
11 Maris JM, Hogarty MD, Bagatell R, Cohn SL. Neuroblastoma. *Lancet* 2007; **369**: 2106-2120.
12 De Bernardi B, Nicolas B, Boni L, Indolfi P, Carli M, di Montezemolo LC *et al.* Disseminated neuroblastoma in children older than one year at diagnosis: comparable results with three consecutive high-dose protocols adopted by the Italian Co-Operative Group for Neuroblastoma. *J Clin Oncol* 2003; **21**: 1592-1601.
13 Matthay KK, Villablanca JG, Seeger RC, Stram DO, Harris RE, Ramsay NK *et al.* Treatment of high-risk neuroblastoma with intensive chemotherapy, radiotherapy, autologous bone marrow transplantation, and 13-*cis*-retinoic acid. *N Engl J Med* 1999; **341**: 1165-1173.
14 Pearson ADJ, Pinkerton CR, Lewis IJ, Imeson J, Ellershaw C, Machin D *et al.* High-dose rapid and standard induction chemotherapy for patients aged over 1 year with stage 4 neuroblastoma: a randomised trial. *Lancet Oncol* 2008; **9**: 247-256.
15 Beckmann G, Bork P. An adhesive domain detected in functionally diverse receptors. *Trends Biochem Sci* 1993; **18**: 40-41.
16 Loren CE, Englund C, Grabbe C, Hallberg B, Hunter T, Palmer RH. A crucial role for the anaplastic lymphoma kinase receptor tyrosine kinase in gut development in *Drosophila melanogaster*. *EMBO Rep* 2003; **4**: 781-786.
17 Choudhary C, Olsen JV, Brandts C, Cox J, Reddy PNG, Boehmer FD *et al.* Mislocalized activation of oncogenic RTKs switches downstream signaling outcomes. *Mol Cell* 2009; **36**: 326-339.
18 Mazot P, Cazes A, Boutterin MC, Figueiredo A, Raynal V, Combaret V *et al.* The constitutive activity of the ALK mutated at positions F1174 or R1275 impairs receptor trafficking. *Oncogene* 2011; **30**: 2017-2025.
19 Lemmon MA, Schlessinger J. Cell signaling by receptor tyrosine kinases. *Cell* 2010; **141**: 1117-1134.
20 Lu Y, Yao HP, Wang MH. Multiple variants of the RON receptor tyrosine kinase: biochemical properties, tumorigenic activities, and potential drug targets. *Cancer Lett* 2007; **257**: 157-164.
21 Pedersen MW, Meltorn M, Damstrup L, Poulsen HS. The type III epidermal growth factor receptor mutation-biological significance and potential target for anti-cancer therapy. *Ann Oncol* 2001; **12**: 745-760.
22 Ekstrand AJ, James CD, Cavenee WK, Seliger B, Pettersson RF, Collins VP. Genes for epidermal growth-factor receptor, transforming growth factor-alpha, and epidermal growth-factor and their expression in human gliomas *in vivo*. *Cancer Res* 1991; **51**: 2164-2172.
23 Wong AJ, Ruppert JM, Bigner SH, Grzeschik CH, Humphrey PA, Bigner DS *et al.* Structural alterations of the epidermal growth-factor receptor gene in human gliomas. *Proc Natl Acad Sci USA* 1992; **89**: 2965-2969.
24 Gan HK, Kaye AH, Luwor RB. The EGFRvIII variant in glioblastoma multiforme. *J Clin Neurosci* 2009; **16**: 748-754.
25 Prigent SA, Nagane M, Lin H, Huvar I, Boss GR, Feramisco JR *et al.* Enhanced tumorigenic behavior of glioblastoma cells expressing a truncated epidermal growth factor receptor is mediated through the Ras-Shc-Grb2 pathway. *J Biol Chem* 1996; **271**: 25639-25645.
26 Zhou YQ, He C, Chen YQ, Wang D, Wang MH. Altered expression of the RON receptor tyrosine kinase in primary human colorectal adenocarcinomas: generation of different splicing RON variants and their oncogenic potential. *Oncogene* 2003; **22**: 186-197.
27 Ronsin C, Muscatelli F, Mattei MG, Breathnach R. A novel putative receptor protein tyrosine kinase of the met family. *Oncogene* 1993; **8**: 1195-1202.
28 Wang MH, Kurtz AL, Chen YQ. Identification of a novel splicing product of the RON receptor tyrosine kinase in human colorectal carcinoma cells. *Carcinogenesis* 2000; **21**: 1507-1512.
29 Chen YQ, Zhou YQ, Angeloni D, Kurtz AL, Qiang XZ, Wang MH. Overexpression and activation of the RON receptor tyrosine kinase in a panel of human colorectal carcinoma cell lines. *Exp Cell Res* 2000; **261**: 229-238.
30 Palmer RH, Vernersson E, Grabbe C, Hallberg B. Anaplastic lymphoma kinase: signalling in development and disease. *Biochem J* 2009; **420**: 345-361.
31 Chiarle R, Voena C, Ambrogio C, Piva R, Inghirami G. The anaplastic lymphoma kinase in the pathogenesis of cancer. *Nat Rev Cancer* 2008; **8**: 11-23.
32 Schulte JH, Bachmann HS, Brockmeyer B, DePreter K, Oberthur A, Ackermann S *et al.* High ALK receptor tyrosine kinase expression supersedes ALK mutation as a determining factor of an unfavorable phenotype in primary neuroblastoma. *Clin Cancer Res* 2011; **17**: 5082-5092.
33 Takita J, Yang HW, Chen YY, Hanada R, Yamamoto K, Teitz T *et al.* Allelic imbalance on chromosome 2q and alterations of the caspase 8 gene in neuroblastoma. *Oncogene* 2001; **20**: 4424-4432.
34 Brodeur GM, Pritchard J, Berthold F, Carlsen NLT, Castel V, Castleberry RP *et al.* Revisions of the international criteria for neuroblastoma diagnosis, staging, and response to treatment. *J Clin Oncol* 1993; **11**: 1466-1477.
35 Takita J, Hayashi Y, Nakajima T, Adachi J, Tanaka T, Yamaguchi N *et al.* The p16 (CDKN2A) gene is involved in the growth of neuroblastoma cells and its expression is associated with prognosis of neuroblastoma patients. *Oncogene* 1998; **17**: 3137-3143.
36 Donella-Deana A, Marin O, Cesaro L, Gunby RH, Ferrarese A, Coluccia AML *et al.* Unique substrate specificity of anaplastic lymphoma kinase (ALK): development of phosphoacceptor peptides for the assay of ALK activity. *Biochemistry* 2005; **44**: 8533-8542.
37 Smith JL, McBride CM, Nataraj PS, Bartos DC, January CT, Delisle BP. Trafficking-deficient hERG K(+) channels linked to long QT syndrome are regulated by a microtubule-dependent quality control compartment in the ER. *Am J Physiol-Cell Physiol* 2011; **301**: C75-C85.

Supplementary Information accompanies the paper on the Oncogene website (http://www.nature.com/onc)

臨床研究

本邦における小児 Hodgkin リンパ腫 157 例の後方視的検討 —小児がん研究 4 グループによる調査—

古賀友紀[1,2]，熊谷昌明[1,3]，瀧本哲也[1,3]，三間屋純一[1,4]，
中澤温子[1,3]，堀部敬三[1,5]，小林良二[1,6]，鶴沢正仁[1,7]，
稲田浩子[1,8]，森　鉄也[1,3]

Hodgkin リンパ腫は小児がんの中でも予後良好な疾患の一つである。本邦における本疾患の発症は，年間 10 数例と極めて少ないため，これまでにまとまった報告がなされず，臨床的背景などの実態は明らかではなかった。今回，1985～2000 年に小児がん治療研究 4 グループにおいて治療を受けた Hodgkin リンパ腫 157 例を対象として，その臨床的特徴，治療および予後について，後方視的に解析した。157 例の内訳は男 107 例，女 50 例，発症年齢は中央値 10 歳 1 か月（1 歳 8 か月～17 歳 8 か月）であった。病期は I：37 例（24%），II：62（39%），III：40 例（26%），IV：18 例（11%）であり，そのうち B 症状を認めた症例が 50 例（32%）であった。ほとんどの症例が cyclophosphamide, vincristine, procarbazine, prednisolone（COPP），doxorubicin, bleomycin, vinblastine, dacarbazine（ABVD）を用いた化学療法を受けており，125 例（82%）が 6 コース以上施行されていた。5 年無病生存率は 81.5%，全生存率は 94.8%であった。多変量解析により，高リスク，年齢（10 歳以上）が予後不良因子としてあげられた。（臨床血液 53（4）：443～449，2012）

Key words : Hodgkin lymphoma, Children, Retrospective study

はじめに

Hodgkin リンパ腫は，小児・成人領域を含め，欧米では一般的な疾患のひとつであるが，本邦においては悪性リンパ腫の 5～10%にすぎない[1]。これまでに小児 Hodgkin リンパ腫に関するまとまった報告はなく，今日に至るまで統一プロトコールが作成されなかったことから，欧米の優れた臨床試験結果を参考に，各施設において治療がすすめられてきたのが現状である。

今回，日本における小児がん治療研究グループである東京小児がん研究グループ，小児白血病研究会，小児癌白血病研究グループおよび九州・山口小児がん研究グループの計 4 グループで経験した小児 Hodgkin リンパ腫 157 症例を後方視的に調査し，その臨床的特徴，治療および予後について検討した。

受付：2011 年 8 月 30 日
受理：2012 年 1 月 19 日
[1] 日本小児白血病リンパ腫研究グループ
[2] 九州大学病院　小児科
[3] 独立行政法人国立成育医療研究センター
[4] 静岡県熱海健康福祉センター
[5] 独立行政法人国立病院機構名古屋医療センター臨床研究センター
[6] 社会医療法人北楡会札幌北楡病院
[7] 愛知医科大学　小児科
[8] 久留米大学　地域医療連携講座

目的と方法

日本における小児 Hodgkin リンパ腫治療の現状を把握する目的に，以下の 4 グループにおいてアンケート調査を依頼した。対象は東京小児がん研究グループ 39 例（1988～1997 年），小児白血病研究会 66 例（1990～2000 年），小児癌白血病研究グループ 40 例（1985～2000 年）および九州・山口小児がん研究グループ 12 例（1990～2000 年）の計 157 例であり，各グループが独自に行ったアンケート調査結果を 2003 年までに集計した。調査項目は患者臨床背景（性，年齢，病期，B 症状の有無，病理組織型，化学療法の種類・コース数，放射線照射の有無，外科的摘出の有無），予後（無病生存率，全生存率），晩期合併症の種類および観察期間である。病期は Ann Arbor 分類に基づき[2]，最も生存率に差を有した病期群（stage I～IIA，IIB 以上）の 2 つに分け，それぞれを低リスクおよび高リスクと定義し解析を行った。

なお，生存率は Kaplan-Meier 法を用い，log-rank test により統計処理を行い，統計学的バラツキを示すため

に，標準誤差5%範囲（±SE）を示した。また，Cox回帰分析を用いて予後因子の多変量解析を施行した。

結　果

今回検討した157例の臨床背景を（表1）に示す。157例の内訳は男107例，女50例，発症年齢は中央値10歳1か月（1歳8か月～17歳8か月）であった。病期I：37例（24%），II：62例（39%），III：40例（26%），IV：18例（11%）であり，うちB症状を認めた症例が50例（32%）であった。病理組織型はリンパ球豊富型42例（27%），結節硬化型56例（36%），混合細胞型43例（27%），リンパ球減少型5例（3%），その他11例（7%）であった。

治療レジメンは各施設，症例で異なっており，統一されたプロトコールは使用されなかった。治療の特徴を（表2）に示す。化学療法のみで治療施行された例は85例（54%），化学療法および放射線療法併用は67例（43%），放射線療法のみが3例（2%），手術のみが2例（1%）であった。化学療法レジメンは，cyclophosphamide, vincristine, procarbazine, prednisolone（COPP），doxorubicin, bleomycin, vinblastine, dacarbazine（ABVD）療法を施行した症例がほとんどであり（68%），125例（82%）の症例が6コース以上の化学療法を施行されていた。なお，低リスク症例においても，60例（75%）の症例が6コース以上の化学療法を受けていた。また，放射線療法は70例（45%）が受けており（中央値29.7 Gy：10～80 Gy），低リスクの症例においても，41例（59%）が放射線療法を受けていた。

表1　小児Hodgkinリンパ腫・患者背景

	(n=157)	症例数	%
性	男児	107	68
	女児	50	32
年齢	0～4歳	20	13
	5～9歳	52	33
	10～歳	85	54
病期	I	37	24
	II	62	39
	III	40	26
	IV	18	11
	I～IIA	85	54
	IIB～IV	72	46
B症状の有無	無	107	68
	有	50	32
組織分類	リンパ球豊富型	42	27
	結節硬化型	56	36
	混合細胞型	43	27
	リンパ球減少型	5	3
	その他	11	7

全症例（157例）における無病生存率および全生存率を（図1, 2）に示す。生存は147例，死亡は10例（非腫瘍死1例を含む），再発は25例（非寛解2例を含む）であった。5年無病生存率は81.5±3.4%，10年無病生存率は80.2±3.6%，5年全生存率は94.8±1.9%，10年全病生存率は90.0±3.4%であった。

いくつかのサブグループ別に検討した無病生存率を（表3）に示す。男女別の無病生存率はそれぞれ79.2%，86.3%であり，2群間に有意差はみられなかった。病期別ではStage I～IIA 89.7%，Stage IIB～IV 72.6%（p=0.004），B症状の有無では有74.6%，無85.0%（p=0.037），年齢別では10歳未満88.5%，10歳以上75.4%（p=0.027）とそれぞれにおいて有意差が認められた。さらに治療においては放射線療法の有無，化学療法のコース数（6コース未満かそれ以上か）で差は認められなかった。さらに，10歳未満，10歳以上の2群各々において病期，性，放射線照射の有無での無病生存率を検討したところ，10歳以上の群で，高リスク群（p=0.003），男児（p=0.03），放射線非照射例（p=0.04）で生存率が有意に低い結果となった（図3）。特に，10歳以上，高リスクでかつ非照射例（n=23）の無病生存率は47.3%であり，同じ条件の照射例（n=19）の83.6%に比して有意に低かった（p=0.001）。これらの単変量解析に引き続きCox回帰分析による予後因子を多変量解析してみると，年齢10歳以上（p=0.04），病期IIB以上（高リスク）（p=0.02）が有意なリスク因子となった（表4）。照射の有無などの治療因子は予後との相関は認められなかった。

晩期合併症観察期間は平均72±4か月（±SE），中央値66か月（1～233ヵ月）であり，二次がん1例（Desmoid tumor），局所の変形3例（斜頚，下顎の発育障害，側弯症），内分泌障害7例（無月経，甲状腺機能低下，二次性徴遅延，肥満，不妊），心筋障害2例，神経障害1例であった。

考　察

小児Hodgkinリンパ腫は，本疾患の進展様式の特殊性から，浸潤したリンパ節領域を網羅する系統立てた放射線照射（マントル型照射および逆Y字型照射）がながく標準的治療とされていた。1970年代には，mechlorethamine, vincristine, procarbazine, prednisolone（MOPP），ABVD療法という多剤併用化学療法の有効性が示され，

表 2　小児 Hodgkin リンパ腫・治療背景

	小児 Hodgkin リンパ腫（n＝157）	症例数	%
治療の種類	化学療法	85	54
	化学療法＋放射線療法	67	43
	放射線療法	3	2
	外科的摘出	2	1
	化学療法を受けた全患者（n＝152）	症例数	%
化学療法レジメン	COPP（MOPP）	104	68
	ABVD	103	68
	A-COPP	16	11
	COPP/ABV	11	7
	OPEA	53	35
	OPPA	43	28
	その他	4	3
コース数	1～5	27	18
	6	64	42
	7～	61	40
	病期 I～IIA 患者（n＝80）	症例数	%
コース数	1～5	20	25
	6	38	48
	7～	22	27
	病期 IIB～IV 患者（n＝72）	症例数	%
コース数	1～5	7	10
	6	26	36
	7～	39	54
	放射線療法を受けた全患者（n＝70）	症例数	%
病期分類	I～IIA	41	59
	IIB～IV	29	41

COPP＝cyclophosphamide, vincristine, procarbazine, prednisone
MOPP＝mechloretamine, vincristine, procarbazine, prednisone
ABVD＝doxorubicin, bleomycin, vinblastine, dacarbazine
A-COPP＝doxorubicin, cyclophosphamide, vincristine, procarbazine, prednisone
COPP/ABV＝cyclophosphamide, vincristine, procarbazine, prednisone, doxorubicin, bleomycin, vinblastine
OEPA＝vincristine, etoposide, prednisone, doxorubicin
OPPA＝vincristine, prednisone, procarbazine, doxorubicin

放射線照射との併用で高い治癒率が達成された。しかし，1980 年代に抗腫瘍薬および放射線照射による性腺障害，二次がん，心・肺障害などの重篤な晩期合併症，非腫瘍死が報告された。さらに小児期特有の合併症として，成長障害や照射部位の変形が問題となった。したがって，1990 年代より今日に至るまでは，生存率を高く維持しつつ，晩期合併症を減らす（治療を軽減する）ことを目標に欧米を中心に臨床試験が進められた。

ドイツにおける臨床試験 German Society of Pediatric Oncology and Hematology-Hodgkin's Disease（GPOH HD）-95 では[3]，低リスクにおいて 2 コースの OPPA（vincristine, procarbazine, prednisolone, doxorubicin; 女児）

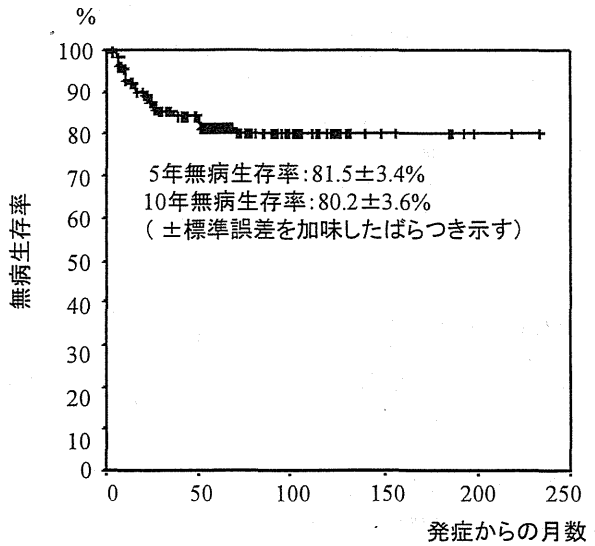

図1 小児 Hodgkin リンパ腫・無病生存率

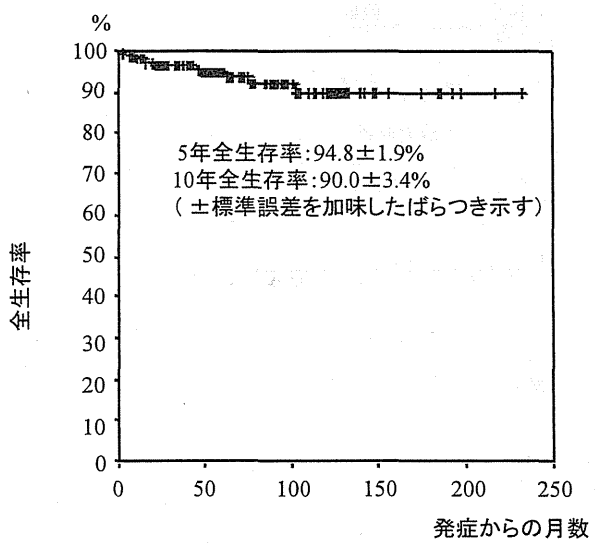

図2 小児 Hodgkin リンパ腫・全生存率

もしくは OEPA（vincristine, etoposide, prednisolone, doxorubicin; 男児）に加え，寛解が得られなかった症例に対してのみ局所照射が行われ，6年無病生存率が94%と非常に良好な成績であった。中間リスクでは計4コースの化学療法 2OEPA/OPPA+2COPP ±局所放射線療法（寛解例は照射を省略），高リスクでは計6コースの化学療法 2OEPA/OPPA+4COPP± 局所放射線療法（寛解例は照射を省略）を施行し，照射・非照射群ともに90%以上の全生存率が得られたが，無病生存率は照射群の方が有意に高かった（中間+高リスク；照射群91%，非照射群81%）。これを元に，GPOH HD-2002 では，低リスクのみ寛解例は照射を省略し，さらに男児の不妊を回避する目的で，男児の procarbazine を撤廃し，etoposide および dacarbazine に変更した[4]。男児と女児で同等の無病生存率が得られ，放射線照射省略による女児の二次発がん，procarbazine 省略による男児の不妊を軽減できる可能性が示唆された。

表3 小児 Hodgkin リンパ腫・5年無病生存率

評価項目		5年無病生存率(%)	P value
性	男児	79.2	0.26
	女児	86.3	
年齢	0～9歳	88.5	0.027
	10～歳	75.4	
病期分類	I～IIA	89.7	0.004
	IIB～IV	72.6	
B症状	無	85.0	0.037
	有	74.6	
放射線照射	無	80.5	0.58
	有	82.5	

Children's Cancer Group（CCG）59704 では[5]，初発時高リスク症例を対象に，4コースの bleomycin, etoposide, doxorubicin, cyclophosphamide, vincristine, procarbazine, prednisolone（BEACOPP）後に初期治療反応性によって治療強度を決定した。Rapid early response の女児では照射を回避する目的で COPP/ABV を4コース，男児ではアルキル化薬を回避する目的で ABVD2 コースののちに放射線照射を施行。5年無病および全生存率ともに94%以上と，これまでの成績を上回る結果が得られた。

Stanford, St Jude and Dana Farber consortium では[6]，低リスク症例に4コースの VAMP（vinblastine, doxorubicin, methotrexate, prednisolone）の後，完全寛解例には15 Gy，部分寛解例には25.5 Gy の照射がなされ，生存率に有意差は認められなかった。照射の軽減が可能であるとともに，低リスクであればアルキル化薬を使用しなくても治癒可能であることが示唆された。高リスクにおいては6コースの VAMP/COP ののちに完全寛解例には15 Gy，部分寛解例には25.5 Gy の照射がなされたが，5年無病生存率75.6%であり，高リスクに対するアルキル化薬減量は十分な結果とはいえないものであった[7]。

このように欧米では放射線照射対象を慎重に減らし，化学療法についても MOPP，ABVD，COPP の組み合わせから OPPA，OPEA，BEACOPP，COPP/ABV，VAMP/COP など，性腺障害や二次がんの発生を抑える薬剤の組み合わせが試みられ，良好な成績を報告している。

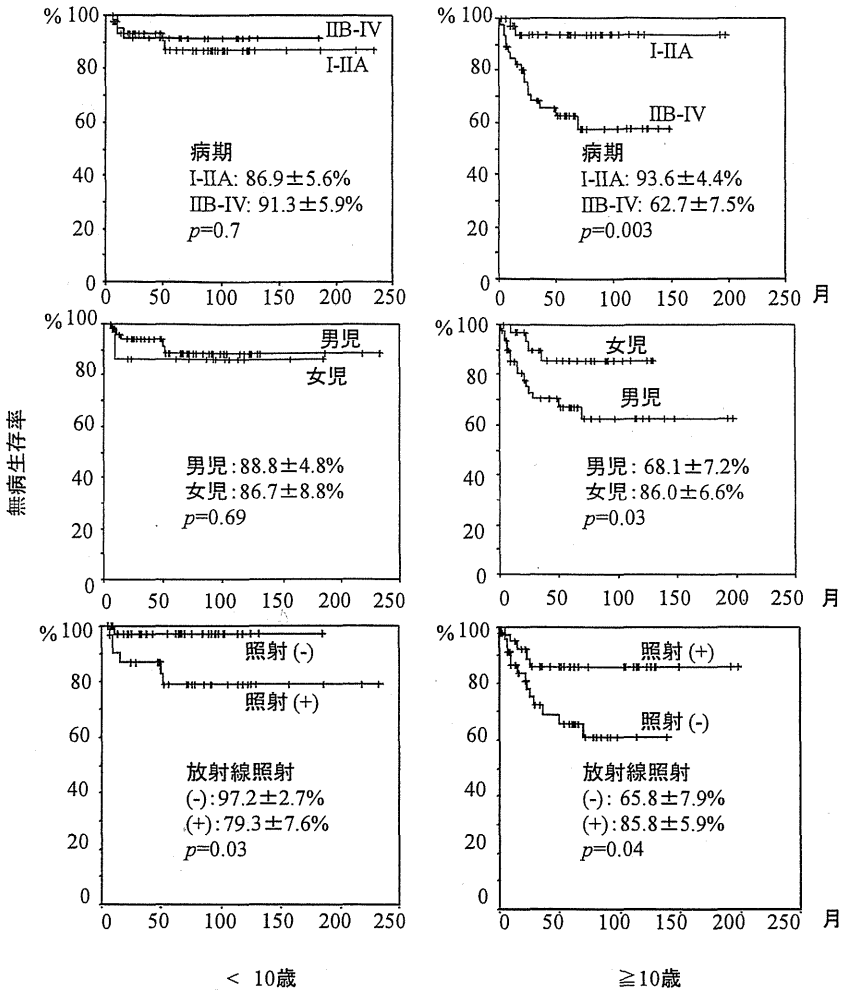

図3 小児 Hodgkin リンパ腫・10 歳未満，10 歳以上における無病生存率
左列：10 歳未満，右列：10 歳以上
横軸：発症からの月数を示す
グラフ内 ±：標準誤差を加味したばらつき示す

表4 小児 Hodgkin リンパ腫・予後因子多変量解析（Cox 回帰分析）

評価項目		回帰係数	リスク比（CI 95%）	P value
性	男児	0.83	2.28（0.90～5.79）	0.08
年齢	10 歳以上	0.92	2.50（1.03～6.09）	0.04
病期	IIB～IV	1.08	2.95（1.19～7.28）	0.02

また，これら臨床試験と同時に，晩期合併症（二次がん，性腺障害，心筋障害）についての大規模な報告も相次いでいる。Bhatia らの 1,380 例の小児 Hodgkin リンパ腫の報告[8]では，二次がん発生率は原病の発症から 15 年間で 7%と報告された（固形腫瘍 3.9%，白血病 2.8%，非 Hodgkin リンパ腫など 0.3%）。また，小児 Hodgkin リンパ腫において，放射線照射（特に 30Gy 以上），アントラサイクリン系薬剤，アルキル化薬は用量依存性に晩期合併症の risk factor になること[9]，さらに小児 Hodgkin リンパ腫において，放射線照射は低用量（15～25.5 Gy）でも二次がんの risk factor になることが報告された[10]。

一方，本邦の小児 Hodgkin リンパ腫臨床試験は今日に至るまで一度も作成・実行されておらず，正確な臨床

背景，治療，予後および晩期合併症などの実態は明らかではなかった。その理由として，本邦における小児Hodgkinリンパ腫の年間発生数が10数例と極めて少ないこと，Hodgkinリンパ腫臨床試験において不妊，二次がん，心筋障害などの合併症を評価項目とする場合，10年以上の経過観察が必要であること，海外の治療プロトコールの優れた治療成績をさらに改善するようなレジメンを作成するならば，結果的に治療を強めることとなり，Hodgkinリンパ腫治療における最大の問題点である晩期合併症を無視せざるを得ないこと，などが挙げられる。

今回の報告は本邦初となる小児ホジキンリンパ腫の後方視的実態調査である。各臨床試験によりリスク分類および治療法が異なるため，治療成績を比較する際には慎重にならざるを得ないが，本邦における生存率は各国と大きな差はないように思われた。しかしながら，生存率以外の点では，残念ながら各国の進んだ臨床研究結果との比較に値するものとはならなかった。化学療法の種類については，各国が性腺障害や二次がんの発生を抑制するべく薬剤の変更や減量を工夫する中，本邦においてはいまだ，各施設間で治療法が統一されておらず，ほとんどが従来型のCOPPあるいはABVD，もしくはその併用療法が用いられていた。化学療法コース数については，病期I～IIAの低リスクにおいても，75%の症例が6コース以上，27%の症例が7コース以上の複数コースの化学療法を施行されていた（高リスクは6コース以上が90%，7コース以上が54%）。放射線照射ついては，低リスクの59%，高リスクの41%が照射対象となり，各国が低リスク寛解例に照射を省略し，高リスクには照射は省略せずに照射野を狭くする努力を行う傾向にある中，本邦においてはむしろ，低リスクの照射対象が多く，高リスクへの照射は半数以下であった。さらに，合併症観察期間は平均72±4か月と短く，晩期合併症の観察期間としては十分と言えるものではなく，合併症発症症例の治療内容の詳細は不明であった。

以上のように，施設間で治療法が統一されていない，心筋障害のリスクにかかわらずABVDを標準とする傾向がある，COPPによる男児の不妊リスクについて理解が少ない，放射線照射の適応，照射野の設定，線量についての統一見解が存在しない，観察期間が短いために晩期合併症の検討が不十分である，などのさまざま点が明らかとなった。

現在，日本小児白血病リンパ腫研究グループ・リンパ腫委員会において，今回の調査で明らかとなった問題点を元に，これまでに達成された高い治癒率を維持しながら，できるかぎり晩期合併症を減少させることを目的として，治療法の検討が行われている。非照射群の適正な設定，前方視的な長期フォローアップシステムの構築，などが重要な課題である。

謝　辞

アンケート調査にご協力くださいました各研究グループ，施設の先生方に深謝いたします。

なお，本調査は故・熊谷昌明先生を中心に尽力され，まとめあげられたものです。この場を借りて深く感謝の意を表するとともに，ご冥福をお祈りいたします。

著者のCOI（conflicts of interest）開示：本論文発表内容に関連して特に申告なし

文　献

1) 鈴宮淳司. ホジキンリンパ腫. 臨血. 2009; **50**: 261-270.
2) Olweny CL. Cotswolds modification of the Ann Arbor staging system for Hodgkin's disease. J Clin Oncol. 1990; **8**: 1598.
3) Rühl U, Albrecht M, Dieckmann K, et al. Response-adapted radiotherapy in the treatment of pediatric Hodgkin's disease: an interim report at 5 years of the German GPOH-HD 95 trial. Int J Radiat Oncol Biol Phys. 2001; **54**: 1209-1218.
4) Mauz-Körholz C, Hasenclever D, Dörffel W, et al. Procarbazine-free OEPA-COPDAC chemotherapy in boys and standard OPPA-COPP in girls have comparable effectiveness in pediatric Hodgkin's lymphoma: the GPOH-HD-2002 study. J Clin Oncol. 2010; **28**: 3680-3686.
5) Kelly KM, Sposto R, Hutchinson R, et al. BEACOPP chemotherapy is a highly effective regimen in children and adolescents with high-risk Hodgkin lymphoma: a report from the Children's Oncology Group. Blood. 2011; **117**: 2596-2603.
6) Donaldson SS, Link MP, Weinstein HJ, et al. Final results of a prospective clinical trial with VAMP and low-dose involved-field radiation for children with low-risk Hodgkin's disease. J Clin Oncol. 2007; **25**: 332-337.
7) Hudson MM, Krasin M, Link MP, et al. Risk-adapted, combined-modality therapy with VAMP/COP and response-based, involved-field radiation for unfavorable pediatric Hodgkin's disease. J Clin Oncol. 2004; **22**: 4541-4550.
8) Bhatia S, Robison LL, Oberlin O, et al. Breast cancer and other second neoplasms after childhood Hodgkin's disease. N Engl J Med. 1996; **334**: 745-751.
9) Castellino SM, Geiger AM, Mertens AC, et al. Morbidity and mortality in long-term survivors of Hodgkin lymphoma: a report from the Childhood Cancer Survivor Study. Blood. 2011; **117**: 1806-1816.
10) O'Brien MM, Donaldson SS, Balise RR, Whittemore AS, Link MP. Second malignant neoplasms in survivors of pediatric Hodgkin's lymphoma treated with low-dose radiation and chemotherapy. J Clin Oncol. 2010; **28**: 1232-1239.

Retrospective analysis of 157 patients with pediatric Hodgkin lymphoma in Japan: investigation by four pediatric cancer study groups

Yuhki KOGA[1,2], Masaaki KUMAGAI[1,3], Tetsuya TAKIMOTO[1,3], Jun-ichi MIMAYA[1,4], Atsuko NAKAZAWA[1,3], Keizo HORIBE[1,5], Ryoji KOBAYASHI[1,6], Masahito TSURUSAWA[1,7], Hiroko INADA[1,8], Tetsuya MORI[1,3]

[1] Japanese Pediatric Leukemia/Lymphoma Study Group
[2] Department of Pediatrics, Kyushu University
[3] National Center for Child Health and Development
[4] Atami Public Health and Welfare Center
[5] Nagoya Medical Center Clinical Research Center
[6] Sapporo Hokuyu Hospital
[7] Department of Pediatrics, Aichi Medical University
[8] Department of Community Medicine, Kurume University School of Medicine

Key words : Hodgkin lymphoma, Children, Retrospective study

Hodgkin lymphoma is an easily curable malignancy in the pediatric age group and is less frequently observed in Japan. No study with a large sample size of Japanese patients has been conducted. From 1985 to 2000, 157 Japanese patients with Hodgkin lymphoma were retrospectively analyzed based on their clinical characteristics, treatment regimen, and treatment outcome by 4 pediatiric cancer study groups. There were 107 male and 50 female patients with a median age of 10 years 1 month (range: 1 year 8 months to 17 years 8 months). Clinical stage I lymphoma was observed in 37 patients, stage II in 62, stage III in 40, and stage IV in 18. Fifty patients presented with B symptoms (32%). Most patients (n=125, 82%) received more than 6 courses of combination chemotherapy mainly comprising cyclophosphamide, vincristine, procarbazine, prednisolone (COPP), doxorubicin, bleomycin, vinblastine, and dacarbazine (ABVD). The 5-year overall and event-free survival rates were 81.5% and 94.8%, respectively. High-risk disease and age (>10 years) were considered to be poor prognostic factors.

Open

Leukemia (2012) 26, 1879–1898

www.nature.com/leu

LETTERS TO THE EDITOR

Novel splicing-factor mutations in juvenile myelomonocytic leukemia

Leukemia (2012) **26,** 1879–1881; doi:10.1038/leu.2012.45

Myelodysplastic syndromes (MDS) and myelodysplastic/myeloproliferative neoplasms (MDS/MPN) are heterogeneous groups of chronic myeloid neoplasms characterized by clonal hematopoiesis, varying degrees of cytopenia or myeloproliferative features with evidence of myelodysplasia and a propensity to acute myeloid leukemia (AML).[1] In recent years, a number of novel gene mutations, involving *TET2*, *ASXL1*, *DNMT3A*, *EZH2*, *IDH1/2*, and *c-CBL*, have been identified in adult cases of chronic myeloid neoplasms, which have contributed to our understanding of disease pathogenesis.[2–7] However, these mutations are rare in pediatric cases, with the exception of germline or somatic *c-CBL* mutations found in 10–15% of chronic myelomonocytic leukemia (CMML) and juvenile myelomonocytic leukemia (JMML),[8] highlighting the distinct pathogenesis of adult and pediatric neoplasms.[9]

Recently, we reported high frequencies of mutations, involving the RNA splicing machinery, that are largely specific to myeloid neoplasms, showing evidence of myeloid dysplasia in adult.[10] Affecting a total of eight components of the RNA splicing machinery (U2AF35, U2AF65, SF3A1, SF3B1, SRSF2, ZRSR2, SF1 and PRPF40B) commonly involved in the 3′ splice-site (3′SS) recognition, these pathway mutations are now implicated in the pathogenesis of myelodysplasia.[10] To investigate the role of the splicing-pathway mutations in the pathogenesis of pediatric myeloid malignancies, we have examined 165 pediatric cases with AML, MDS, chronic myeloid leukemia (CML) and JMML for mutations in the four major splicing factors, *U2AF35*, *ZRSR2*, *SRSF2*, and *SF3B1*, commonly mutated in adult cases.

Bone marrow or peripheral blood tumor specimens were obtained from 165 pediatric patients with various myeloid malignancies, including *de novo* AML ($n=93$), MDS ($n=28$), CML ($n=17$) and JMML ($n=27$), and the genomic DNA (gDNA) was subjected to mutation analysis (Supplementary Table 1). The status of the RAS pathway mutations for the current JMML series has been reported previously (Supplementary Table 2).[11,12] Nineteen leukemia cell lines derived from AML (YNH-1, ML-1, KASUMI-3, KG-1, HL60, inv-3, SN-1, NB4 and HEL), acute monocytic leukemia (THP-1, SCC-3, J-111, CTS, P31/FUJ, MOLM-13, IMS/MI and KOCL-48) and acute megakaryoblastic leukemia (CMS and CMY) were also analyzed for mutations. Peripheral blood gDNA from 60 healthy adult volunteers was used as controls. Informed consent was obtained from the patients and/or their parents and from the healthy volunteers. We previously showed that for *U2AF35*, *SRSF2* and *SF3B1*, most of the mutations in adult cases were observed in exons 2 and 7, exon 1, and exons 14 and 15, respectively.[10] Therefore, we confirmed mutation screening to these 'hot-spot' exons. In contrast, all the coding exons were examined for *ZRSR2*, because no mutational hot spots have been detected. Briefly, the relevant exons were amplified using PCR and mutations were examined by Sanger sequencing, as previously described.[10] The Fisher's exact test was used to evaluate the statistical significance of frequencies of mutations for *U2AF35*, *SF3B1*, *ZRSR2* or *SRSF2* in adult cases and pediatric cases. This study was approved by the Ethics Committee of the University of Tokyo (Approval number 948-7).

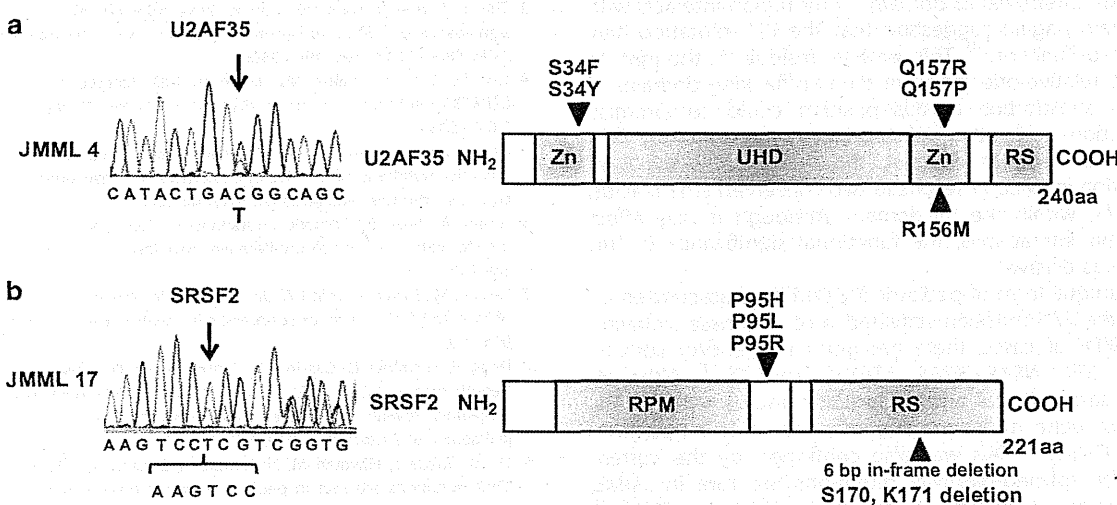

Figure 1. Novel *U2AF35*and *SRSF2* mutations detected in JMML cases. (**a**) Left panel: sequence chromatogram of a heterozygous mutation at R156 in N-terminal zinc-finger motifs of *U2AF35* detected in a JMML case (JMML 4) is shown. Mutated nucleotides are indicated by arrows. Right panel: illustration of functional domains and mutations of U2AF35. Red arrow heads indicate hot-spot mutations at S34 and Q157 detected in the adult cases.[10] Blue arrow head indicates the missense mutation at R156. (**b**) Left panel: sequence chromatogram of a 6-bp in-frame deletion (c.518-523delAAGTCC) in *SRSF2* detected in JMML 17 is shown. Mutated nucleotides are indicated by arrows. Right panel: illustration of functional domains and mutations of SRSF2. Red arrow head indicates hot-spot mutation at P95 frequently detected in the adult cases.[10] Blue arrow head indicates a 6-bp in-frame deletion leading to deletion of S170 and K171.

Accepted article preview online 20 February 2012; advance online publication, 2 March 2012

No mutations were identified in the 28 cases with pediatric MDS, which included 13 cases with refractory anemia with excess blasts, 5 with refractory cytopenia of childhood, 2 with Down syndrome-related MDS, 2 with Fanconi anemia-related MDS, 2 with secondary MDS and 4 with unclassified MDS. Similarly, no mutations were detected in 93 cases with *de novo* AML or in 17 with CML, as well as 19 leukemia-derived cell lines. Our previous study in adult patients showed the frequency of mutations in *U2AF35*, *SF3B1*, *ZRSR2* or *SRSF2* to be 60/155 cases with MDS without increased ring sideroblasts and 8/151 *de novo* AML patients, emphasizing the rarity of these mutations in pediatric MDS ($P<5.0\times10^{-6}$) and AML ($P<0.02$) compared with adult cases. We found mutations in two JMML cases, JMML 4 and JMML 17. JMML 4 carried a heterozygous *U2AF35* mutation (R156M), whereas JMML 17 had a 6-bp in-frame deletion (c.518-523delAAGTCC) in *SRSF2* that resulted in deletion of amino acids S170 and K171 (Figure 1). Both nucleotide changes found in *U2AF35* and *SRSF2* were neither identified in the 60 healthy volunteers nor registered in the dbSNP database (http://www.ncbi.nlm.nih.gov/projects/SNP/) or in the 1000 genomes project, indicating that they represent novel spliceosome mutations in pediatric cases.

U2AF35 is the small subunit of the U2 auxiliary factor (U2AF), which binds an AG dinucleotide at the 3′SS, and has an essential role in RNA splicing.[13] With the exception of a single A26V mutation found in a case of refractory cytopenia with multilinage dysplasia, all the U2AF35 mutations reported in adult myeloid malignancies involved one of the two hot spots within the two zinc-finger domains, S34 and Q157, which are highly conserved across species, suggesting the gain-of-function mutations.[10] In JMML 4, the R156M U2AF35 mutation affects a conserved amino acid adjacent to Q157, suggesting it may also be a gain-of-function mutation, leading to aberrant pre-mRNA splicing possibly in a dominant fashion.

SRSF2, better known as SC35, is a member of the serine/arginine-rich (SR) family of proteins.[14] SRSF2 binds to a splicing-enhancer element in pre-mRNA and has a crucial role not only in constitutive and alternative pre-mRNA splicing but also in transcription elongation and genomic stability.[14] All mutations thus far identified in adult cases exclusively involved P95 within the intervening sequence between the N-terminal RNA-binding domain and the C-terminal RS domain.[10] This region interacts with other SR proteins, again suggesting that the P95 mutation may result in gain-of-function.[10] This proline residue is thought to determine the relative orientation of the two flanking domains of SRSF2, and a substitution at this position could compromise critical interactions with other splicing factors necessary for RNA splicing to take place. In contrast, the newly identified 6-bp in-frame deletion in JMLL 17 results in two conserved amino acids, S170 and K171, within the RS domain. Although it may affect protein–protein interactions, the functional significance of this deletion remains elusive.

JMML is a unique form of pediatric MDS/MPN characterized by activation of the RAS/mitogen-activated protein kinase signaling pathway; in 90% of cases, there are germ line and/or somatic mutations of *NF1*, *NRAS*, *KRAS*, *PTPN11* and *CBL*.[8] Although JMML shares some clinical and molecular features with CMML, its spectrum of gene mutations suggests that it is a neoplasm distinct from CMML.[15] This was also confirmed by the current results that the splicing-pathway mutations are rare in JMML, whereas they are extremely frequent (~60%) in CMML.[10] Although the two JMML cases carrying the splicing-pathway mutations had no known RAS-pathway mutations, both the pathway mutations frequently coexisted in CMML.[8]

To summarize, no mutations of *SF3B1*, *U2AF35*, *ZRSR2* or *SRSF2* are found in pediatric MDS and AML. In our study, except for *ZRSR2*, mutations were examined focusing on the reported hot spots in adult studies, raising a possibility that we may have missed some mutations occurring in other regions. However, these hot spots represent evolutionally conserved amino acids and have functional relevance, it is unlikely that the distribution of hot spots in children significantly differs from adult cases and as such, we could safely conclude that mutations of *SF3B1*, *U2AF35*, *ZRSR2* and *SRSF2* are rare in myeloid neoplasms in children. Finally, mutations of *U2AF35* and *SRSF2* may have some role in the pathogenesis of JMML, although further evaluations are required.

CONFLICT OF INTEREST

The authors declare no conflict interest.

ACKNOWLEDGEMENTS

This work was supported by Research on Measures for Intractable Diseases, Health and Labor Sciences Research Grants, Ministry of Health, Labor and Welfare, by Research on Health Sciences focusing on Drug Innovation, and the Japan Health Sciences Foundation. We would like to thank M Matsumura, M Yin, N Hoshino and S Saito for their excellent technical assistance.

J Takita[1,2], K Yoshida[3], M Sanada[3], R Nishimura[1], J Okubo[1], A Motomura[1], M Hiwatari[1], K Oki[1], T Igarashi[1], Y Hayashi[4] and S Ogawa[3]

[1]*Department of Pediatrics, Graduate School of Medicine, The University of Tokyo, Tokyo, Japan;*
[2]*Department of Cell Therapy and Transplantation Medicine, Graduate School of Medicine, The University of Tokyo, Tokyo, Japan;*
[3]*Cancer Genomics Project, Graduate School of Medicine, The University of Tokyo, Tokyo, Japan and*
[4]*Gunma Children's Medical Center, Gunma, Japan*
E-mail: sogawa-tky@umin.ac.jp

REFERENCES

1 Garcia-Manero G. Myelodysplastic syndromes: 2011 update on diagnosis, risk-stratification, and management. *Am J Hematol* 2011; **86**: 490–498.
2 Delhommeau F, Dupont S, Della Valle V, James C, Trannoy S, Masse A *et al.* Mutation in TET2 in myeloid cancers. *N Engl J Med* 2009; **360**: 2289–2301.
3 Thol F, Friesen I, Damm F, Yun H, Weissinger EM, Krauter J *et al.* Prognostic significance of ASXL1 mutations in patients with myelodysplastic syndromes. *J Clin Oncol* 2011; **29**: 2499–2506.
4 Ley TJ, Ding L, Walter MJ, McLellan MD, Lamprecht T, Larson DE *et al.* DNMT3A mutations in acute myeloid leukemia. *N Engl J Med* 2010; **363**: 2424–2433.
5 Nikoloski G, Langemeijer SM, Kuiper RP, Knops R, Massop M, Tonnissen ER *et al.* Somatic mutations of the histone methyltransferase gene EZH2 in myelodysplastic syndromes. *Nature Genet* 2010; **42**: 665–667.
6 Green A, Beer P. Somatic mutations of IDH1 and IDH2 in the leukemic transformation of myeloproliferative neoplasms. *N Engl J Med* 2010; **362**: 369–370.
7 Sanada M, Suzuki T, Shih LY, Otsu M, Kato M, Yamazaki S *et al.* Gain-of-function of mutated C-CBL tumour suppressor in myeloid neoplasms. *Nature* 2009; **460**: 904–908.
8 Perez B, Kosmider O, Cassinat B, Renneville A, Lachenaud J, Kaltenbach S *et al.* Genetic typing of CBL, ASXL1, RUNX1, TET2 and JAK2 in juvenile myelomonocytic leukaemia reveals a genetic profile distinct from chronic myelomonocytic leukaemia. *Br J Haematol* 2010; **151**: 460–468.
9 Oki K, Takita J, Hiwatari M, Nishimura R, Sanada M, Okubo J *et al.* IDH1 and IDH2 mutations are rare in pediatric myeloid malignancies. *Leukemia* 2011; **25**: 382–384.
10 Yoshida K, Sanada M, Shiraishi Y, Nowak D, Nagata Y, Yamamoto R *et al.* Frequent pathway mutations of splicing machinery in myelodysplasia. *Nature* 2011; **478**: 64–69.
11 Chen Y, Takita J, Hiwatari M, Igarashi T, Hanada R, Kikuchi A *et al.* Mutations of the PTPN11 and RAS genes in rhabdomyosarcoma and pediatric hematological malignancies. *Genes Chromosomes Cancer* 2006; **45**: 583–591.
12 Shiba N, Kato M, Park MJ, Sanada M, Ito E, Fukushima K *et al.* CBL mutations in juvenile myelomonocytic leukemia and pediatric myelodysplastic syndrome. *Leukemia* 2010; **24**: 1090–1092.

Oncogene (2012) **31,** 4667–4676

www.nature.com/onc

ORIGINAL ARTICLE

Aberrant activation of ALK kinase by a novel truncated form ALK protein in neuroblastoma

J Okubo[1], J Takita[1,2], Y Chen[1], K Oki[1], R Nishimura[1], M Kato[1], M Sanada[3], M Hiwatari[1], Y Hayashi[4], T Igarashi[1] and S Ogawa[3]

Anaplastic lymphoma kinase (ALK) was originally identified from a rare subtype of non-Hodgkin's lymphomas carrying t(2;5)(p23;q35) translocation, where ALK was constitutively activated as a result of a fusion with nucleophosmin (NPM). Aberrant ALK fusion proteins were also generated in inflammatory fibrosarcoma and a subset of non-small-cell lung cancers, and these proteins are implicated in their pathogenesis. Recently, ALK has been demonstrated to be constitutively activated by gene mutations and/or amplifications in sporadic as well as familial cases of neuroblastoma. Here we describe another mechanism of aberrant ALK activation observed in a neuroblastoma-derived cell line (NB-1), in which a short-form ALK protein (ALK^{del2-3}) having a truncated extracellular domain is overexpressed because of amplification of an abnormal *ALK* gene that lacks exons 2 and 3. ALK^{del2-3} was autophosphorylated in NB-1 cells as well as in ALK^{del2-3}-transduced cells and exhibited enhanced *in vitro* kinase activity compared with the wild-type kinase. ALK^{del2-3}-transduced NIH3T3 cells exhibited increased colony-forming capacity in soft agar and tumorigenicity in nude mice. RNAi-mediated ALK knockdown resulted in the growth suppression of ALK^{del2-3}-expressing cells, arguing for the oncogenic role of this mutant. Our findings provide a novel insight into the mechanism of deregulation of the ALK kinase and its roles in neuroblastoma pathogenesis.

Oncogene (2012) **31,** 4667–4676; doi:10.1038/onc.2011.616; published online 16 January 2012

Keywords: neuroblastoma; *ALK*; truncated form ALK; amplification

INTRODUCTION

Anaplastic lymphoma kinase (ALK) (OMIM: 105590) is an orphan receptor tyrosine kinase (RTK) that was initially characterized as a fusion partner of the nucleophosmin (NPM)-ALK chimeric protein associated with the t(2;5)(p23;q35) translocation in anaplastic large-cell lymphoma.[1,2] Subsequent studies have revealed that various ALK-containing fusion proteins with different fusion partners are generated in various solid tumors, such as inflammatory myofibroblastic tumors, non-small-cell lung cancer and squamous cell carcinoma of the esophagus.[3–6] Furthermore, recent genome-wide studies have revealed that *ALK* is activated by gene amplification and nucleotide mutations and is involved in the pathogenesis of both familial and sporadic neuroblastoma.[7–10]

Neuroblastoma is an intractable, solid tumor of childhood arising from the neural crest and can arise anywhere along the sympathetic nervous system.[11] The overall 5-year survival rate for neuroblastoma is ⩽40%, despite current intensive multimodality treatments.[12–14] Considering that *ALK* mutations preferentially involve advanced neuroblastoma with a poor outcome, the more relevant implication of these findings is that ALK inhibitors may improve the clinical outcome of children suffering from intractable neuroblastoma.

In this study, we demonstrated another mechanism of aberrant ALK activation in neuroblastoma, in which an abnormal *ALK* gene with a deletion of exons 2 and 3 was amplified in a neuroblastoma-derived cell line (NB-1), leading to high-level expression of an ALK protein variant with a truncated extracellular domain (ALK^{del2-3}). Furthermore, we demonstrated that ALK^{del2-3} had constitutive kinase activity and showed a transforming capacity in NIH3T3 cells. Moreover, ALK inhibition experiments using small interfering RNA (siRNA)-mediated gene knockdown and the low-molecular-weight compound, TAE684, also supported the oncogenic role of ALK^{del2-3}. Our results will help elucidate the mechanism of aberrant activation of ALK kinase and the role of activated ALK in the pathogenesis of neuroblastoma.

RESULTS

Detection of a short-form ALK protein in NB-1 cells

To examine the status of ALK in neuroblastoma, western blotting analysis was performed with a panel of 24 neuroblastoma-derived cell lines (Table 1). Among the 24 samples examined, the NB-1 cell line showed high-level expression of an ALK protein having a low molecular weight of 208 kDa compared with the molecular weight of 220 kDa for the wild-type protein (Figure 1a). Subsequent sequencing and reverse transcription–polymerase chain reaction (RT–PCR) analysis of *ALK* messages from NB-1 cells revealed the presence of an aberrant *ALK* transcript with a 285-bp in-frame deletion in the 5′ region corresponding to exons 2 and 3 (Figures 1b and c), which should result in the production of an abnormal ALK protein with a truncated N-terminal extracellular domain. Using a primer set for exons 2 and 3, a 166-bp product was also detected in NB-1 cells, indicating the presence of the wild-type *ALK* allele in NB-1 cells (Figures 1b and c). The deletion spanned 224–318 amino acids (aa), including the N-terminal end of the first meprin A5 protein and receptor protein tyrosine phosphatase mu (MAM) domain (aa 264–427) (Figure 1d).[15,16] We analyzed full-length *ALK* cDNAs isolated from 71 primary neuroblastoma samples for possible nucleotide deletions using RT–PCR (Table 2), but no deletions were detected.

[1]Department of Pediatrics, Graduate School of Medicine, University of Tokyo, Tokyo, Japan; [2]Department of Cell Therapy and Transplantation Medicine, Graduate School of Medicine, University of Tokyo, Tokyo, Japan; [3]Cancer Genomics Project, Graduate School of Medicine, University of Tokyo, Tokyo, Japan and [4]Gunma Children's Medical Center, Maebashi, Japan. Correspondence: Dr J Takita, Cell Therapy and Transplantation Medicine, Graduate School of Medicine, University of Tokyo, 7-3-1, Hongo, Bunkyo-ku, Tokyo 113-8655, Japan. E-mail: jtakita-tky@umin.ac.jp
Received 22 May 2011; revised and accepted 29 November 2011; published online 16 January 2012

Table 1. Neuroblastoma cell lines used in this study

Cell line	*MYCN amplification*	*ALK status*
CHP-134	–	WT
GOTO	+	WT
LAN-1	+	F1174L
LAN-2	+	WT
LAN-5	+	R1275Q
NB-1	–	Amplification
NB-16	+	WT
NB-19	+	WT
NB-69	–	WT
NH-12	+	WT
SCMC-N2	+	F1174L
SCMC-N4	+	WT
SCMC-N5	+	K1062M
SJNB-1	–	WT
SJNB-2	+	R1275Q
SJNB-3	–	WT
SJNB-4	+	F1174L
SJNB-5	+	WT
SJNB-6	+	WT
SJNB-7	+	WT
SJNB-8	+	WT
SK-N-SH	–	F1174L
TGW	+	R1275Q
UTP-N-1	+	WT

Abbreviations: ALK, anaplastic lymphoma kinase; WT, wild type.

Structural abnormality of the *ALK* gene in NB-1 cells

As reported previously,[7] our single-nucleotide polymorphism array-based copy number analysis of NB-1 cells disclosed high-level gene amplification of the *ALK*-containing 2p24 segment. This should explain the high *ALK* expression observed in this cell line (Figures 1a and b). In particular, the genomic copy numbers within the 2p23 amplicon exhibited a transient decrease at three consecutive single-nucleotide polymorphisms (Chr2: 29 911 541–29 912 210), which corresponded to *ALK* intron 3, raising the possibility that a gene deletion involving exons 2 and 3 was responsible for the aberrant *ALK* transcript (Figure 2a). To confirm this, we performed Southern blot analysis of NB-1 genomic DNA using fragments exons 1–4 as probes (Figure 2b). As shown in Figures 2c–e, Southern blot analysis confirmed *ALK* gene amplification in NB-1 cells, as these blots showed high-intensity signals for each of the four *ALK*-specific probes in NB-1 cells compared with those in the controls. However, a significant difference was observed in the signal intensity between the fragments containing exons 1/4 and exons 2/3 in the NB-1 lanes, in which exons 1 and 4 showed 3.9- and 3.8-fold higher signals than exons 2 and 3, respectively. This result was confirmed by quantitative genomic PCR analysis using seven primer sets located within *ALK* exons 1–4 (Figure 2f). Taken together, these results indicate that the 2p23 amplicons were heterogeneous with regard to the species of *ALK* it contained, among which the predominant *ALK* allele had a deletion at exons 2 and 3, and these amplicons were responsible for the generation of $ALK^{del2\text{-}3}$.

Oncogenic potential of an aberrant short-form ALK protein

We next evaluated the oncogenic role of the truncated form of ALK found in NB-1 cells in terms of its kinase activity. As shown in Figure 3a, $ALK^{del2\text{-}3}$ was strongly phosphorylated in NB-1 cells, whereas the wild-type ALK expressed in NH-12 cells was unphosphorylated. Similar to the constitutive active F1174L ALK mutant when expressed in NIH3T3 cells, $ALK^{del2\text{-}3}$ had enhanced ALK phosphorylation compared with wild-type ALK (Figure 3b). Moreover, after anti-FLAG immunoprecipitation of FLAG-tagged ALK constructs, $ALK^{del2\text{-}3}$ and F1174L ALK mutants were strongly phosphorylated according to western blot analysis using a PY20 blot (Figure 3c). In addition, they exhibited enhanced kinase activity in an *in vitro* kinase assay using the YFF peptide as a substrate (Figure 3d). To confirm kinase activity of the $ALK^{del2\text{-}3}$ mutant, we further examined *in vitro* kinase activities of wild-type and mutant ALK-expressing NIH3T3 cells using a universal substrate. The immunoprecipitated FLAG-tagged $ALK^{del2\text{-}3}$ mutant showed significantly increased kinase activity (Supplementary Figure S1).

In an analysis of activated downstream signaling, significantly enhanced STAT3 phosphorylation was observed in $ALK^{del2\text{-}3}$ and F1174L mutants, whereas a significant increase in AKT phosphorylation was not detected in any samples (Figure 3e and Supplementary Figure S2). Extracellular regulated kinase (ERK) was probably phosphorylated in the F1174L mutant and wild-type ALK, but not in $ALK^{del2\text{-}3}$ (Figure 3e). The results of three independent experiments were quantified by densitometric scanning (Supplementary Figure S2).

We investigated the oncogenic potential of the $ALK^{del2\text{-}3}$ mutant in NIH3T3 cells, in terms of colony formation in soft agar and tumor generation in nude mice. As shown in Figures 4a and b, NIH3T3 cells that were stably transduced with $ALK^{del2\text{-}3}$ and ALK^{F1174L} produced a significantly higher numbers of colonies in soft agar than mock or wild-type *ALK*-transduced cells (Figures 4a and b). When inoculated into nude mice, the $ALK^{del2\text{-}3}$-transduced NIH3T3 cells invariably developed into subcutaneous tumors (5/5), whereas the mock and wild-type *ALK*-transfected cells did not develop into tumors (0/5) (Figure 4c).

$ALK^{del2\text{-}3}$ was retained in the endoplasmic reticulum

Among ALK signaling pathway molecules, STAT3 was only strongly phosphorylated by $ALK^{del2\text{-}3}$, suggesting that the $ALK^{del2\text{-}3}$ mutant was exclusively involved in the STAT3 pathway. It has been previously reported that intracellular fms-like tyrosine kinase-internal tandem duplication activation induces an aberrant downstream signaling outcome.[17] To determine whether $ALK^{del2\text{-}3}$ expresses at the cell surface and mediates signals from endoplasmic reticulum (ER), we analyzed localization and deglycosidation of $ALK^{del2\text{-}3}$ in NB-1 cells and wild-type ALK in NH-12 cells. Immunofluorescence staining revealed that ALK in NB-1 cells was almost colocalized with PDI, whereas ALK in NH-12 cells was largely located at the plasma membrane (Figure 5a). As shown in Supplementary Figure S4, colocalization of ALK and PDI was quantified using the Pearson's correlation coefficient. Moreover, to determine whether $ALK^{del2\text{-}3}$ was subjected to maturation of its oligosaccharides, we examined the endoglycosidase H sensitivity of ALK expressed in NB-1 and NH-12 cells. As shown in Figure 5b, $ALK^{del2\text{-}3}$ in NB-1 cells revealed the high sensitivity of endoglycosidase H compared with the wild-type ALK in NH-12 cells, suggesting that intercellular localization of $ALK^{del2\text{-}3}$ was associated with a defect in N-linked glycosylation.[18] These results indicate that $ALK^{del2\text{-}3}$ is mainly located at ER and aberrantly activates the STAT3 pathway from there.

Effect of ALK inhibition on cell growth in NB-1 cells

Finally, we examined the effect of ALK inhibition on NB-1 cell proliferation using the small-molecule ALK inhibitor TAE684 and siRNA-mediated ALK knockdown. NB-1 cell growth was effectively inhibited by TAE684 with a half maximal inhibitory concentration (IC_{50}) of 13 nM, which was similar to the IC_{50} for SK-N-SH (49 nM; an *ALK*-mutated TAE684-sensitive neuroblastoma cell line), but substantially lower than the IC_{50} for TGW cells with the ALK^{R1275Q} mutant (310 nM), the glioblastoma-derived cell line H4 with wild-type ALK (190 nM) and NIH3T3 cells with no ALK expression (380 nM) (Figure 6a). Similarly, siRNA-mediated knockdown of $ALK^{del2\text{-}3}$ in NB-1 cells resulted in significant suppression of cell proliferation compared with controls transfected with nonspecific